

ENVIRONMENTAL PROTECTION AGENCY

OFFICE OF ENFORCEMENT

EPA 330/3-74-001

*EVALUATION OF
ITT RAYONIER, INC. OUTFALL
PORT ANGELES HARBOR
WASHINGTON*

NATIONAL FIELD INVESTIGATIONS CENTER-DENVER
DENVER, COLORADO

DECEMBER 1974



ENVIRONMENTAL PROTECTION AGENCY
OFFICE OF ENFORCEMENT

EVALUATION OF
ITT RAYONIER, INC. OUTFALL
PORT ANGELES HARBOR
WASHINGTON

NATIONAL FIELD INVESTIGATIONS CENTER - DENVER
DENVER, COLORADO

DECEMBER 1974

CONTENTS

I.	INTRODUCTION	1
	ITT RAYONIER DISCHARGES TO THE HARBOR.	1
	OTHER DISCHARGES TO THE HARBOR	5
II.	SUMMARY AND CONCLUSIONS.	7
III.	PREVIOUS STUDIES	11
	STUDY I: POLLUTION EFFECTS OF PULP AND PAPER MILL WASTE ^{1/}	12
	STUDY II: OUTFALL LOCATION STUDIES - PORT ANGELES HARBOR ^{2/}	13
	NATIONAL OCEANOGRAPHIC DATA CENTER	30
	STORET DATA	33
IV.	REMOTE SENSING STUDY	37
	DROGUE (CURRENT) STUDY	38
	WATER QUALITY DATA (GROUND TRUTH).	41
	RESULTS OF DROGUE STUDY.	44
	ANALYSIS OF EFFLUENT CONCENTRATIONS.	51
	ITT RAYONIER DISCHARGES ALONG SHORE.	57
	CROWN ZELLERBACH CORPORATION	60
V.	MODELING PORT ANGELES HARBOR	65
	MODELING ASSUMPTIONS	65
	THEORY VS. OBSERVATION	70
	EVALUATION OF THE MODEL.	73
	REFERENCES	80
	APPENDIX A: REMOTE SENSING TECHNIQUES	81
	APPENDIX B: TIME-DISTANCE DATA: 24 APRIL 1973 FLIGHTS.	97

TABLES

III-1	Tidal Velocities and Headings	19
III-2	Rhodamine WT Concentrations	23-24
IV-1	Tide Phase Data at Port Angeles	37
IV-2	Ground Truth Data, Port Angeles Harbor.	43
IV-3	Meteorological Data	44
IV-4	Crown Zellerbach Corporation Flow Data.	60
V-1	Calculated Values of Frictional Depth and Current Velocity.	71
V-2	Climatological Summary.	75

FIGURES

I-1	Port Angeles Harbor Location Map.	2
I-2	Port Angeles Harbor Contour Map	3
III-1	Current Meter Stations.	14
III- 2-4	Variability of ITT Rayonier Station Data in Sampling Depth and Number of Observations.	15-17
III- 5,6	Dye Tracer Studies (ITT Rayonier)	21,22
III- 7-10	Drogue Releases	26-29
III-11	Oceanographic Stations in the Strait of Juan de Fuca.	31
III-12	Predicted Discharge Characteristics of the Outfall for the SSL.	34
IV-1	Tide Conditions and Duration of Flights	39
IV-2	Drogue Assembly	40
IV-3	Water Quality Data Stations	42
IV- 4-8	Drogue Vector Diagrams (NFIC-D)	45-42
IV-9	Zone of Dilution for the ITT Rayonier Submerged Diffuser	53
IV-10	Plume from the ITT Rayonier Submerged Diffuser.	54
IV-11	Isoconcentration Diagram of ITT Rayonier Plume.	56
IV-12	Thermal Infrared Map of ITT Rayonier Waste Plume.	58
IV-13	Thermal Infrared Map of Port Angeles Harbor and ITT Rayonier Discharges.	59
IV-14	Crown Zellerbach Corporation Discharges	61
IV-15	Plume of Discoloration in Strait of Juan de Fuca from Crown Zellerbach Corp.	62
V-1	Vertical Structure of a Pure Current.	68
V-2	Vertical Structure in Drift Currents.	69
V-3	Adjustment of the Current Vector.	78

CONVERSIONS

<i>multiply</i> <u>Metric Unit</u>	<i>by</i> <u></u>	<i>to find</i> <u>English Unit</u>
Celsius (°C)	. . . 9/5 (then + 32); or 9/5 (for absolute value)	. . Fahrenheit (°F)
centimeters (cm) 0.394	inches (in.)
kilograms (kg) 2.205	pounds (lb)
kilometers (km) 0.621	miles (mi)
meters (m) 3.281	feet (ft)
meters/second (m/sec) 1.94	knots (kn)
millimeters (mm) 0.039	inches (in.)
cubic meters/day (m ³ /day)	. . . (264 x 10 ⁻⁶)	million gallons/day
metric tons (met. tons) 1.102	short tons (ton; 2,000 lb)

ABBREVIATIONS

BOD	biochemical oxygen demand	mg/l	milligrams/liter
DO	dissolved oxygen	min	minute
hr	hour	mrad	milliradian
IRLS	infrared line scanner	PBI	Pearl-Benson Index
JTU	jackson turbidity units	ppm	parts per million
μm	micrometer	SSL	spent sulfite liquor
μmho/cm	micromhos/centimeter	TSS	total suspended solids

I. INTRODUCTION

Port Angeles Harbor fronts the city of Port Angeles, Wash. on the Strait of Juan De Fuca midway between Seattle and the Pacific Ocean [Fig. I-1]. The Harbor is separated from the Strait by Ediz Hook, a narrow peninsula about 4.8 km (3 mi) long [Fig. I-2]. Harbor width varies from about 0.8 km (0.5 mi) at the closed west end to 2.4 km (1.5 mi) at the east end which opens to the Strait. Water depths range from 10 m (33 ft) near shore to 49 m (161 ft) near Ediz Hook.

ITT RAYONIER DISCHARGES TO THE HARBOR

At the east end of Port Angeles Harbor is the ITT Rayonier, Inc. pulp and paper mill [Fig. I-2]. The mill has five outfalls along the shore with effluents consisting mostly of process and cooling water. And the mill has a submerged (extended) outfall which discharges an ammonia-base hot caustic extract and bleach plant effluent. The outfall also discharges 20 percent of the plant's total ammonia-base spent sulfite liquor (SSL) wasteload; the remaining 80 percent of the SSL is burned at the plant site. The total wasteload discharged by the submerged outfall is 18,100 to 22,700 kg (40,000 to 50,000 lb) per day of biochemical oxygen demand (BOD).

The submerged outfall began operation in August 1972. At that time the Washington State Department of Ecology established a three-dimensional

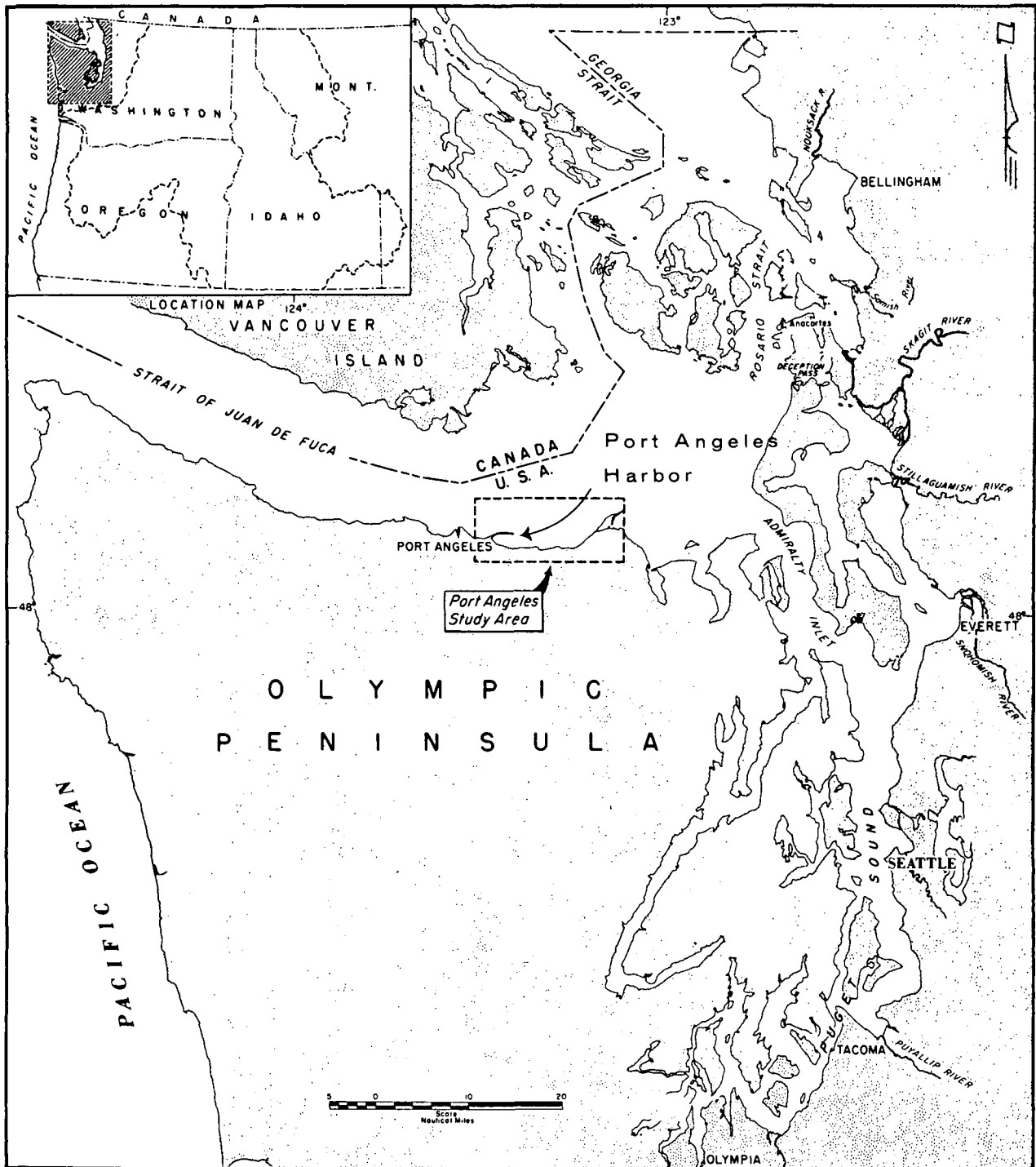


**Figure 1-1. Port Angeles Harbor Location Map
(Modified from Ref. 1.)**

dilution zone surrounding the outfall diffuser measuring 378 m (1,240 ft) long, 155 m (510 ft) wide, and 18 m (60 ft) deep (detailed in Fig. IV-9). The State requires that the effects of chemical and thermal (0.28°C or 0.5°F maximum temperature increase above ambient) wastewater pollutants must not be discernible in the receiving waters outside this zone.

The purpose of this study was to document, using optical and thermal sensors, the dilution or dispersion characteristics of the diffuser effluent as a function of various tide conditions. The study was to answer the following questions:

1. Did the effluent completely disperse within the dilution zone?
2. Did the effluent always disperse to the Strait of Juan de Fuca if it was not completely diluted within the zone?
3. Did the effluent enter Port Angeles Harbor if it did not completely disperse within the zone?

The results of this study will be used by EPA Region X and the Washington State Department of Ecology in assessing the performance of the extended outfall when reissuing the ITT Rayonier NPDES discharge permit.

OTHER DISCHARGES TO THE HARBOR

Other major discharges to Port Angeles Harbor and the Strait of Juan de Fuca were observed during the April and July 1973 remote sensing flights. This minor portion of the study documented the presence and visual behavior of the active discharges discussed below.

Crown Zellerbach Corporation operates a pulp and paper mill at the west end of Ediz Hook. Mill capacity is about 360 met. tons (400 tons) of pulp and 480 tons (435 met. tons) of newsprint daily. Wastewater averaging $34,000 \text{ m}^3/\text{day}$ (9 mgd) is discharged to the Strait of Juan de Fuca and pollutants from this mill would be substantially diluted before entering the circulation patterns of the Harbor. The facility also discharges $10,200 \text{ m}^3/\text{day}$ (2.7 mgd) of wastewater to the Harbor.

Formerly discharged without treatment, the municipal wastewaters from the city of Port Angeles (population about 16,000) are now discharged to the Harbor through a deepwater outfall after primary treatment.

Fibreboard Paper Products Corporation formerly operated a sulfite pulp and board mill near the west end of the Harbor. With a capacity of about 170 met. tons (190 tons) per day, the mill discharged about $15,000 \text{ m}^3/\text{day}$ (4 mgd) of wastewater to the Harbor.

II. SUMMARY AND CONCLUSIONS

The ITT Rayonier pulp and paper facility at Port Angeles, Wash., installed a submerged outfall diffuser [Fig. I-2] in August 1972 to discharge spent sulfite liquor, spent bleach and ammonia hot caustic extract to the waters of Port Angeles Harbor. The total load discharged through this outfall ranges from 18,100 to 22,700 kg (40,000 to 50,000 lb) biochemical oxygen demand per day. Twenty percent of the total SSL discharged from this facility is disposed through the submerged outfall; the remaining 80 percent is incinerated at the plant.

In 1972 the Washington State Department of Ecology established a zone of dilution around this diffuser, requiring that the effluent mix to undetectable levels before leaving the zone. In addition, temperature of the waters leaving this zone must be no warmer than 0.28°C (0.5°F) above that of the receiving waters.

Remote sensing flights over Port Angeles Harbor on 24 April and 25 July 1973 were designed to study the current of the waters emerging from the immediate vicinity of the submerged outfall. A diagram was derived for various concentration levels of wastes from the submerged outfall to document dispersion characteristics of ITT Rayonier's effluent into the Harbor receiving waters.

The current study included five flights, three on 24 April 1973 and two on 25 July 1973. Drogue assemblies were used to monitor the current

and displacement of water at three preassigned depths and at the surface. Two of the three April flights showed that the drogues released near the diffuser moved further into the Harbor (1.5 km; 4,900 ft) rather than dispersing directly to the Strait of Juan de Fuca as planned in the diffuser design and location. During the third flight the drogues did move north beyond Ediz Hook into the Strait. The first flight of July showed the drogues moving in a southwesterly direction further into the Harbor. The last July flight indicated that the effluent would have traveled into the Strait passing close to the east end of Ediz Hook; this flight was terminated before the drogues reached Ediz Hook.

From the airborne data recorded during the first 24 April flight, isoconcentration levels were determined for the diffuser effluent in the Harbor's near-surface waters. Full strength effluent samples obtained from the ITT Rayonier plant at the time of flight were spectroscopically tested and used for optical calibration of the airborne imagery. The highest concentration in the effluent plume, almost directly above the diffuser, was approximately 12 percent of the full-strength sample. The plume extended from the vicinity of the diffuser nearly 1.5 km (0.9 mi) westward into the Harbor before disappearing (displaying optical characteristics identical to those of background water). The plume extended through the upper and the west dilution zone boundaries, resulting in a violation of the State requirements.

The airborne thermal data showed that in the zone of dilution the plume was as much as 1.0°C (1.8°F) cooler than the surface temperature of the receiving water. Thus the plume did not exceed the thermal limitation of 0.28° ((0.5°F) maximum temperature increase at the boundaries of the zone.

ITT Rayonier has five shoreline discharges. A cooling water flow of 14,800 m³/day (3.9 mgd) was being discharged, creating a moderately sized thermal plume during the 25 July flight.

The Crown Zellerbach Corporation operates a pulp and paper plant at the west end of Port Angeles Harbor. The plant discharges wastewater to the Strait of Juan de Fuca and to Port Angeles Harbor through eight outfalls, creating a large yellow plume along the Strait's southern shore.

The National Field Investigations Center - Denver (NFIC-D) analyzed available oceanographic literature on Port Angeles Harbor and found the predicted performance of the ITT Rayonier submerged outfall as described in their study^{2/} to be erroneous. This conclusion is based on an analysis of physical and chemical data, and the dispersion and circulation characteristics in the vicinity of the submerged outfall. However, NFIC-D found correct the conclusion reached by the Federal Water Pollution Control Administration and Washington State Pollution Control Commission report^{1/} which described a weak cyclonic (counterclockwise) motion in Port Angeles Harbor.

A review of all available physical observations indicates that a complicated flushing pattern exists within the Harbor which eliminates a simple gradient current as a possible model. Rather, the observations show that for a significant amount of time a drift current model fits the data, particularly when wind velocities were known.

The factor controlling circulation in Port Angeles Harbor is the wind stress which introduces an Ekman spiral (change in current direction with depth). As a result, water enters the Harbor on the north side, both at the surface and upwelling from depths, and moves out of the Harbor in a cyclonic motion along the south shore. Wastes from the outfall may be carried westward or southward initially. But ultimately they drift eastward along the shore until they reach Green Point or Dungeness Spit and gradually move into the Strait of Juan de Fuca.

The EPA studies indicate that the pollutants discharged through the diffuser can have a long residence in the Harbor. The extended outfall and submerged diffuser is not performing as anticipated by design and is deemed unacceptable. Therefore, the effluent must be treated to a level that will continually meet the requirements in the zone of dilution for all tidal conditions before it is discharged to Port Angeles Harbor.

III. PREVIOUS STUDIES

Two previous studies provide the basis for analyzing the water current patterns near the ITT Rayonier outfall in Port Angeles Harbor.

"Pollution Effects of Pulp and Paper Mill Waste in Puget Sound," ^{1/} includes both an oceanographic survey of current patterns and a water quality study of the Harbor. It concludes that the dominant cyclonic (counterclockwise) eddy motion in the Harbor is generated by currents in the Strait of Juan de Fuca and is superimposed upon weak tidal currents. Also, pulp and paper mill wastes are damaging to marine life in the area. The report recommends construction of a submarine outfall.

The other study, "Outfall Locations Studies -- Port Angeles, Washington" ^{2/} (1970) by ITT Rayonier, Inc. considers chemical, physical and biological parameters, current drogues, and dye studies in determining tidal current patterns and the optimum location of the submarine outfall. The report indicates that the location chosen would not harm water quality. It concludes that the dominant current pattern in the Harbor is an anticyclonic (clockwise) eddy with its center lying east of the midpoint of the entrance to the Harbor.

The conflict in the conclusions of the two reports concerning flushing characteristics and resultant pollution potential within the Harbor has been reviewed in depth. Data in addition to that in the above reports were obtained from the National Oceanographic Data Center (NORDAC) to further document water density and dilution characteristics in Port Angeles Harbor. The analysis of these data follows.

STUDY I: "POLLUTION EFFECTS OF PULP AND PAPER MILL WASTE" ^{1/}

This report contains only a generalized description of the current patterns observed during the first of fourteen oceanographic cruises in the Port Angeles area. The cruises were conducted at approximately monthly intervals between September 1962 and January 1964 to determine water quality. The report concludes that the dominant cyclonic eddy motion generated by currents in the Strait of Juan de Fuca develops near shore between Ediz Hook and Dungeness Spit 13 km (8 mi) to the east. The current transports the water alongshore counter to the main currents in the Strait. It will be shown later that such an eddy circulation can result from the predominant westerly wind and lack of vertical water density stratification in the Port Angeles area.

The report also notes that due to interaction and resonance in the Puget Sound basin, the flood and ebb of currents in the Strait of Juan de Fuca were not necessarily in phase with their respective counterparts at Port Angeles. That such a small geographic area as the Port Angeles Harbor has a complicated current and tidal pattern compared to the laminar flow of the much larger Strait of Juan de Fuca may seem unusual. However, eddy motion in fluids is far more complex and subject to more perturbations than the current in laminar flow.

Local near-surface currents in the Strait of Juan de Fuca were reported as generally less than 1 m/sec (2 kn) in magnitude in an ebb direction primarily due to the seaward movement of fresh water inflow to the Puget Sound basin. Because there are no significant local fresh-water sources in the Port Angeles area, the vertical density gradient is much more gradual than in other areas of Puget Sound.

STUDY II: "OUTFALL LOCATION STUDIES - PORT ANGELES HARBOR" ^{2/}

The ITT Rayonier study reported that the chemical and biological parameters of Port Angeles Harbor had been extensively studied and that current drogue and dye studies had been conducted. The study included 114 hr of current meter observations, taping of 82 hr of continuous current meter readings, and 1,498 individual drogue sightings.

In direct contrast to the first report, this study concludes that the dominant circulation pattern in the Harbor is an anticyclonic eddy with its center lying just east of the midpoint of the entrance to the Harbor.

The current studies performed by ITT Rayonier represent many hours of actual measurement. However, there are many limitations in interpretation because the measurements were brief and intermittent. For the four stations established [Fig. III-1] no current roses* are provided for Station 4, the site of the outfall and thus of great interest. The other three stations were sampled 12 days in July, August and September 1970. Recording time was brief, usually 10 min, with generally an hour or more between observations. The number of observations and the sampling depths varied from one observation day to another.

Typical examples of the variability are shown in Figures III-2 through 4. Since no synoptic current data were taken, generalizations of current patterns are of little value -- such as the vector analysis done on the current roses in Figures III-2 through 4. An examination of Figure III-4 shows that the current was moving in all points of the

* A rose is the card of a mariner's compass.

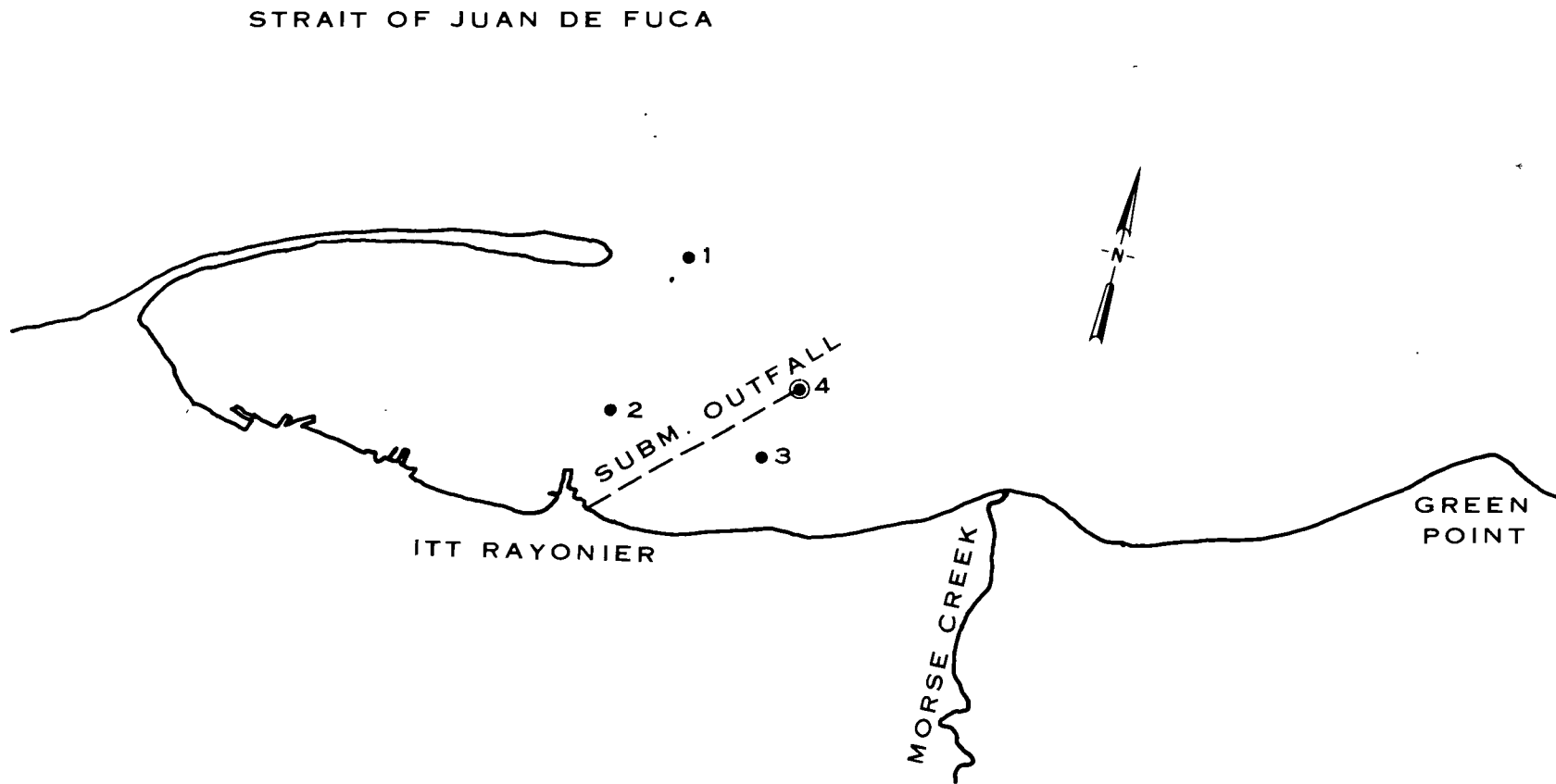
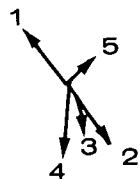
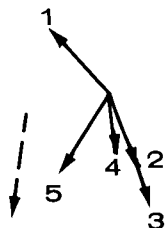


Figure III-1. Current Meter Stations 2/

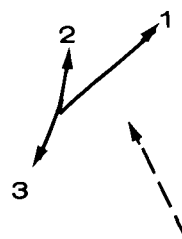
2 meters @ 0915 - 1110 hr



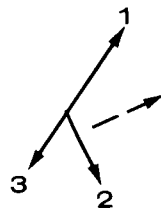
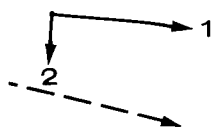
4 meters @ 0930 - 1125 hr



8 meters @ 0950 - 1125 hr



10 meters @ 0930 - 1100 hr



13.5 meters @ 0915 - 1110 hr

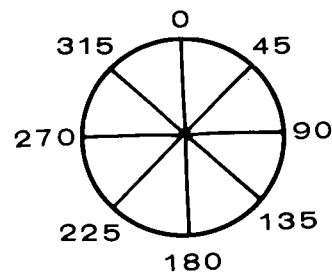


Figure III-2. Variability of ITT Rayonier Station Data in Sampling Depth and Number of Observations (Sta. 1, 7/31/70 2/)

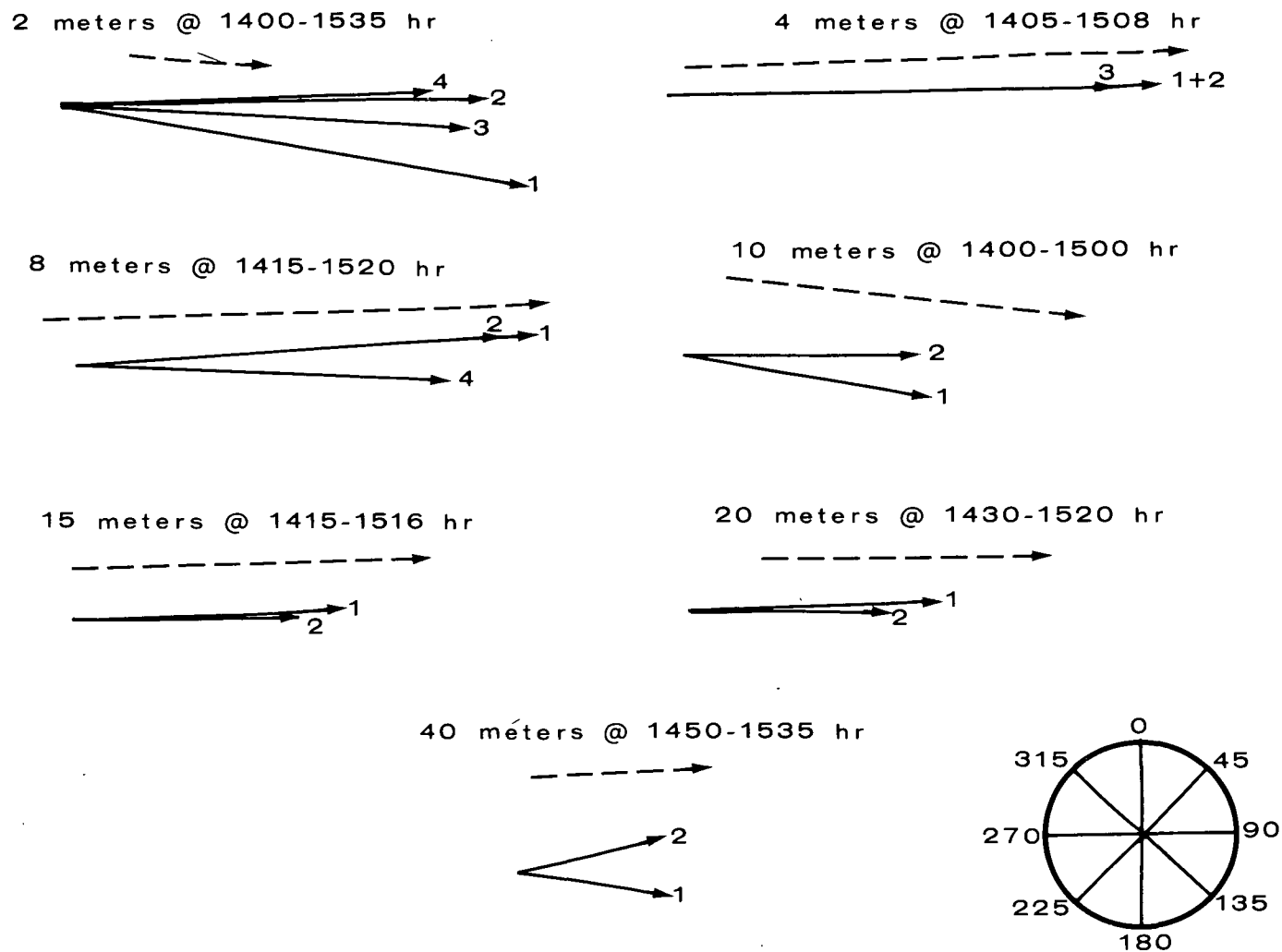


Figure III-3. Variability of ITT Rayonier Station Data in Sampling Depth and Number of Observations (Sta. 1, 8/17/70 2/)

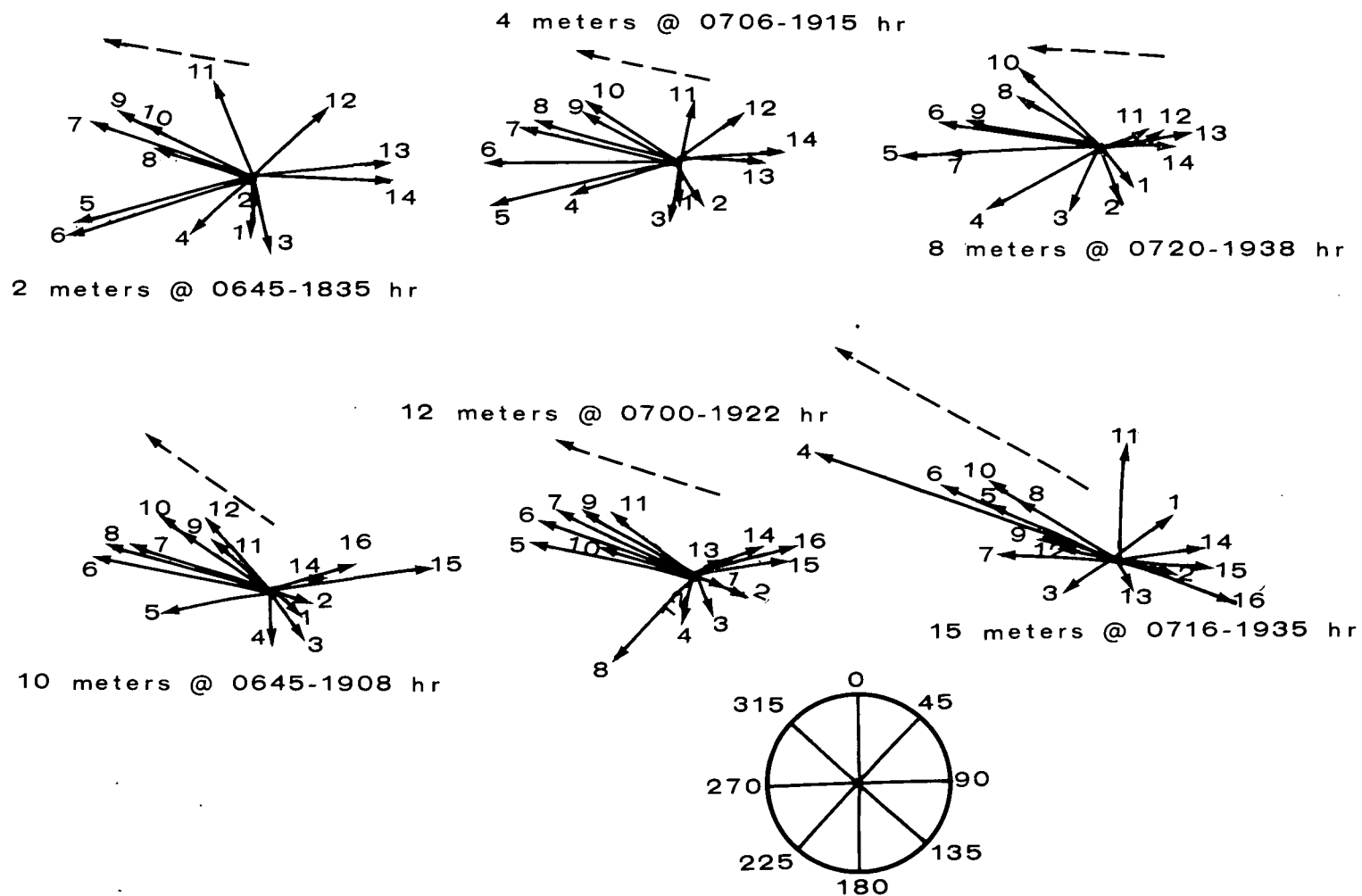


Figure III-4. Variability of ITT Rayonier Station Data in Sampling Depth and Number of Observations (Sta. 2, 8/13/70 2/)

compass during the observation period. Summing the vectors provides no real indication of the water movement. In only one case was there less than a 90° rotation of current direction in the upper layers during the observation period. However, only four observations were made at this particular station on that date, thus limiting the chances of discovering rotation of current direction in the water column. These current observations do not support the report's conclusion that the outfall discharge will be carried out of the Harbor into the Strait of Juan de Fuca most of the time.

Current velocities and headings were continuously recorded at each of the four stations on only a few select days, and then only at the 10 m (33 ft) depth. Since the recorder had not been calibrated until work was finished on Stations 1 and 2, data from those stations have been discarded from further consideration here. A typical set of observations is given in Table III-1. From this limited number of observations it is apparent that the transition from one current direction to another occurs smoothly. The table shows that from 1408 to 1508 hours the current vector changes from a stable heading of essentially 110° to 200° in a smooth incremental manner. The abrupt change of this station noted initially (344° to 20° to 100° in about 10 min) may indicate passage of a frontal system. However, without meteorological data it is not possible to determine coupling, if any, between the atmosphere and the water.

TABLE III-1

TIDAL VELOCITIES AND HEADINGS^{a/}

[Obtained from the Continuous Recording Current Meter
on 31 [sic.] Sept. 1970, from a depth of 10 m at Station 3.]

Time of Observation		1 m/sec = 2 knots .5 m/sec = 1 "	Current Heading (Mag.°)	Time of Observation		Velocity (m/sec)	Current Heading (Mag.°)
from	to	Velocity (m/sec)		from	to		
0915	1058	No ticks recorded		1312	1314	0.12	108
1058	1102	0.14	344	1314	1326	0.13	108
1102	1104	0.13	20	1326	1330	0.11	108
1104	1108	0.15	100	1330	1334	0.10	109
1108	1110	0.18	102	1334	1338	0.08	109
1110	1112	0.16	105	1338	1344	0.10	109
1112	1116	0.14	105	1344	1348	0.12	109
1116	1122	0.17	105	1348	1350	0.17	110
1122	1126	0.18	106	1350	1400	0.10	110
1126	1132	0.19	107	1400	1404	0.11	109
1132	1136	0.17	108	1404	1048[sic.]	0.09	109
1136	1138	0.15	108	1408	1416	0.10	110
1138	1144	0.16	108	1416	1426	0.12	114
1144	1148	0.14	108	1426	1430	0.11	123
1148	1152	0.13	109	1430	1432	0.13	130
1152	1156	0.11	109	1432	1438	0.11	138
1156	1158	0.10	109	1438	1444	0.14	154
1158	1204	0.12	110	1444	1450	0.11	169
1204	1206	0.13	110	1450	1454	0.09	176
1206	1208	0.10	110	1454	1456	0.10	182
1208	1212	0.09	110	1456	1504	0.16	182
1212	1216	0.07	110	1504	1508	0.13	182
1216	1218	0.10	110	1508	1512	0.08	200
1218	1226	0.09	110	1512	1514	0.11	200
1226	1236	0.07	110	1514	1516	0.09	200
1236	1238	0.10	114	1516	1524	0.07	212
1238	1242	0.11	115	1524	1528	0.14	212
1242	1244	0.13	114	1528	1534	0.15	212
1244	1250	0.11	110	1534	1538	0.16	212
1250	1252	0.13	109	1538	1542	0.13	212
1252	1258	0.10	109	1542	1544	0.14	212
1258	1304	0.11	109	1544	1546	0.10	212
1304	1308	0.14	109	1546	1605	0.14	212
1308	1312	0.13	109				

^{a/} Data obtained from ITT Rayonier report^{2/}

Four dye tracer studies traced the transport of an individual parcel of surface water. The dye was released from a point midway between the plant and the outfall and in three cases the dye moved east as it approached the shore. From its initial release point approximately 2.4 km (1.5 mi) off shore, the water parcel moved to within 0.8 km (0.5 mi) of shore, then to about 2.4 km (1.5 mi) east near the entrance to Morse Creek [Fig. III-5]. The fourth release [Fig. III-6] occurred under different tidal conditions. The dye was not carried directly into the Strait of Juan de Fuca. These dye studies do not support the assertion that wastes from the proposed outfall would be carried to the Strait without contaminating the Harbor or the shoreline.

Dye dispersion studies were also performed on the discharge from the City of Port Angeles sanitary waste outfall. The results indicated that the plume did not always reach the surface. Coupled with the diverse movement within the water column, this would indicate that a significant portion of the discharge might be carried into the Harbor at some depth while water at the surface is moving out of the Harbor. Table III-2 gives the results of the rhodamine dye injections discussed in the report. At a point 7.9 m (26 ft) laterally from an outfall discharge port and 4.6 m (15 ft) above it -- an actual linear distance of 9.0 m (30 ft) from the discharge port -- the mean dye concentration was 90 parts per billion in contrast to 11.8 parts per billion at the ^{water} surface. Twice the plume did not reach the surface. The data show that this could not have been caused by density stratification, or a thermocline through which the plume could not penetrate, because the decrease in temperature with depth was very uniform without sharp breaks.

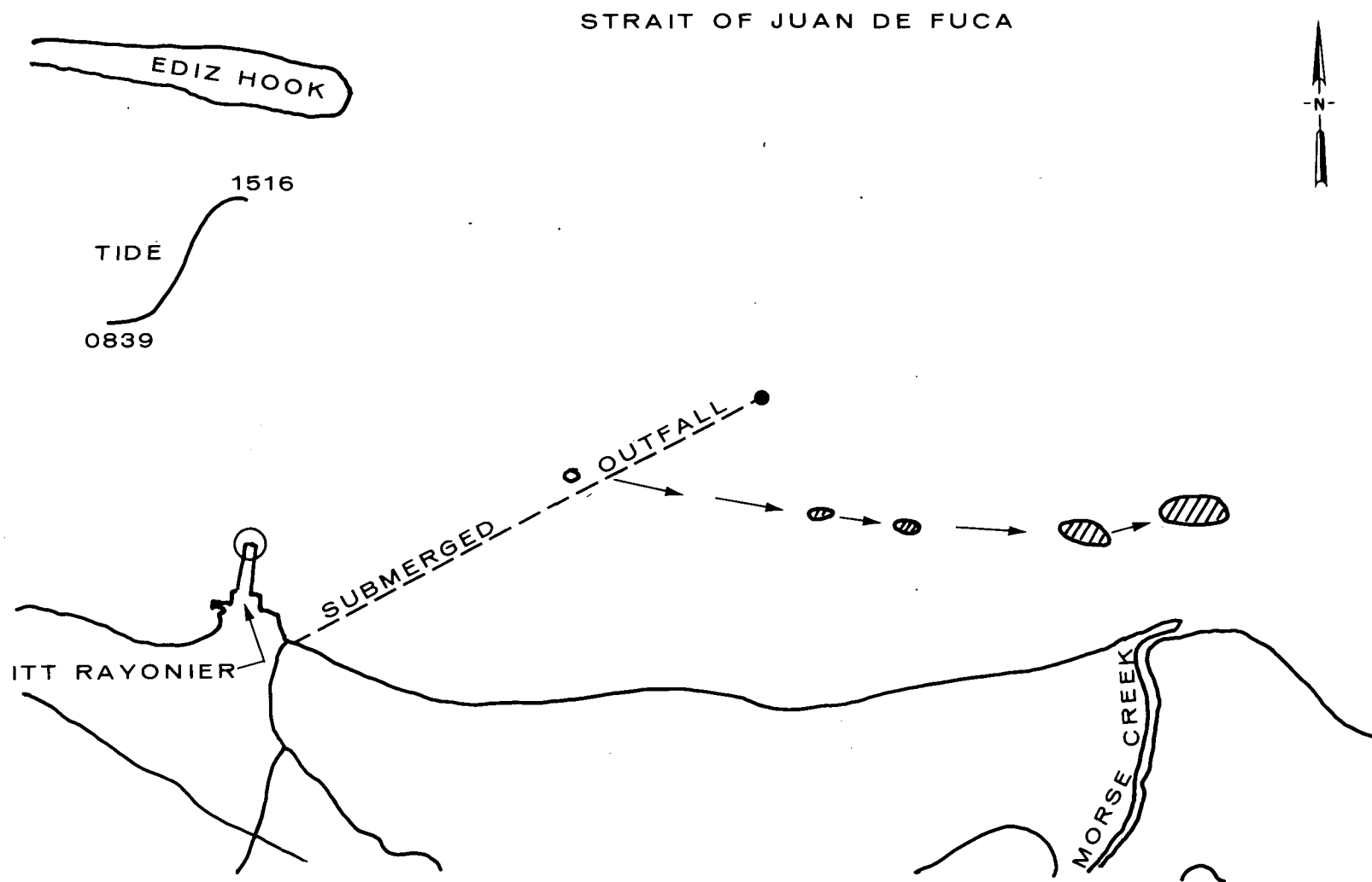


Figure III-5. Dye Tracer Studies (ITT Rayonier, 9/29/70 ²)

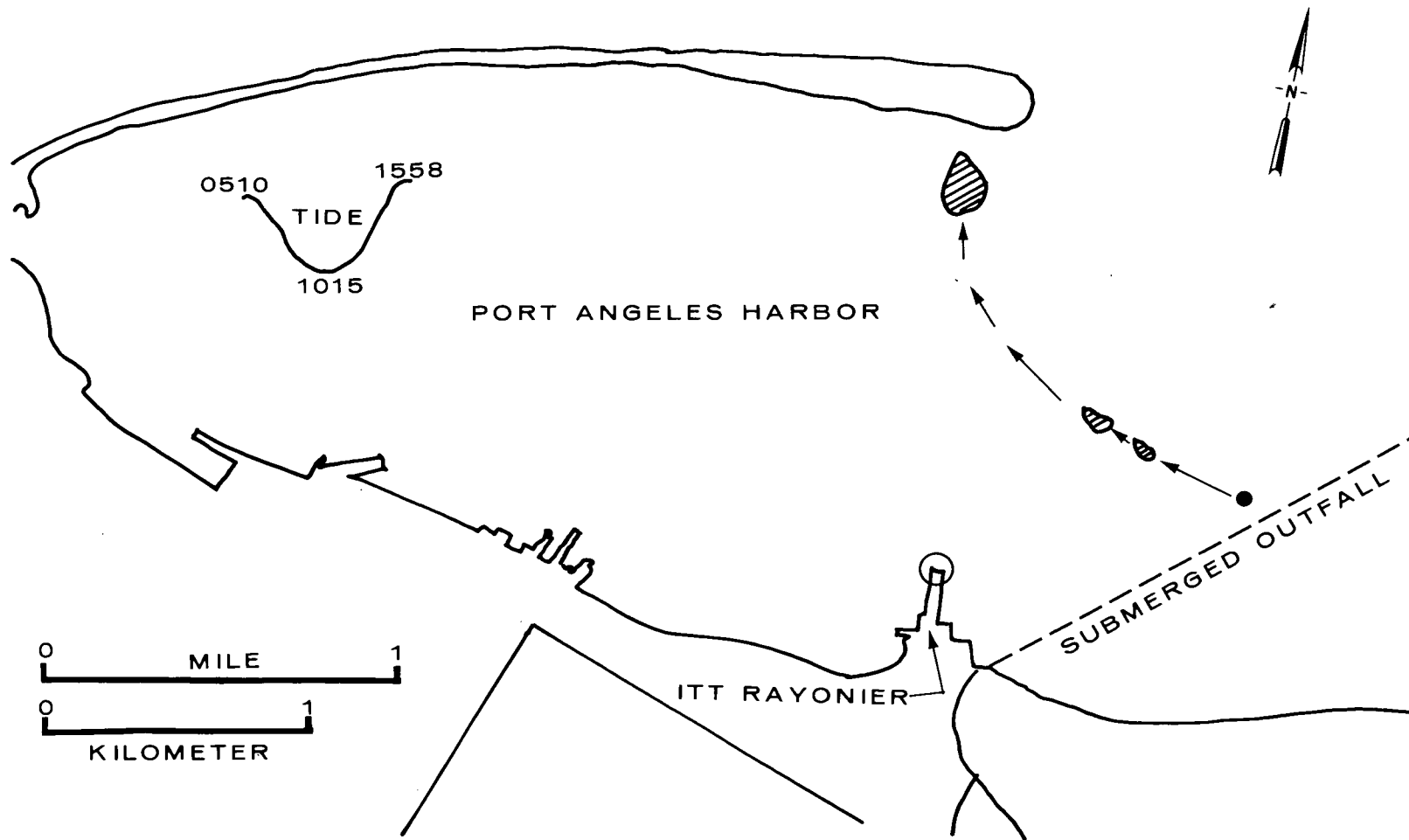


Figure III-6. Dye Tracer Studies (ITT Rayonier, 10/2/70 2/)

Table III-2
Rhodamine WT Concentrations ^{a/}
[Port Angeles City Outfall Study, Oct. 1969]

from port (lateral)	Distance in feet		from surf. (vertical)	Conc. (ppb)	Mean Conc. (ppb)
	above port (vertical)	from port (Σ angular)			
Oct. 22, 1969 - 1658-1706 hr, bearing 320° Mag. - port velocity 4.10 ft/sec - wind W at 5-6 kn					
0	0	0	55	2,900 (off curve)	2,900
8.7	5	10	50	131	131
17.3	10	20	45	128	128
26.0	15	30	40	116 64	90
34.6	20	40	35	79 65	72
45.8	20	50	35	35 42	38.5
63.2	30	70	25	37.0 17.0	27.0
77.4	55	95	0	7.5 16.0	11.8

Plume with surface boil

Oct. 23, 1969 - 1640-1653 hr, bearing 0° Mag. - port velocity 5.73 ft/sec - wind dead calm					
0	0	0	55	2,280 2,350	2,315
5.2	3	6	52	170 194	182
8.7	5	10	50	150 95	122
11.2	10	15	45	60 66	63
8.7	18	20	37	10.4 20.5	15.4
26.0	15	30	40	35.5 37.0* 45.0*	35.5
31.2	25	40	30	38.0 39.0* 50.0*	38.0
44.7	40	60	15	25.0 18.2	21.6
51.0	55	75	0	7.9 7.5	7.7

Plume with surface boil

Table III-2 (cont.)
Rhodamine WT Concentrations
[Port Angeles City Outfall Study, Oct. 1969]

from port (lateral)	Distance in feet		from surf (vertical)	Conc. (ppb)	Mean Conc. (ppb)
	above port (vertical)	from port (Σ angular)			
Oct. 22, 1969 - 1658-1706 hr, bearing 320° Mag. - port velocity 4.10 ft/sec - wind W at 5-6 kn					
0	0	0	60	2,350 2,350	2,350
3.3	5	6	55	320 211	266
12.5	10	16	50	57.0 81.0	69.0
47.7	15	50	45	33.0 30.0	31.5
72.3	20	75	40	13.8	13.8
74.8	25	85	35	6.1 8.6	7.4
98.0	20	100	40	10.9 9.2	10.0
148.7	20	150	40	3.0 3.8	3.4
150.0	60	162	0	2.5 0	1.2

Plume did not surface

Oct. 23, 1969 - 1340-1357 hr, bearing 280° Mag. - port velocity 3.90 ft/sec - wind dead calm					
0	0	0	60	2,450 2,600	2,525
14.1	5	15	55	155	155
28.3	10	30	50	110	110
49.0	10	50	50	30	30
69.3	10	70	50	17.0 36.5	26.8
79.4	10	80	50	12.8 23.8	18.3
99.5	10	100	50	10.1 12.2	11.2
199.0	20	200	40	7.5 8.6	8.0

Plume did not surface

^{a/} Data obtained from ITT Rayonier report ^{2/}

Since the report demonstrates that there was significant current velocity in all directions at depth, a major portion of pollution discharge never reaches the surface. Thus, while the report concludes that water movement near the entrance to Port Angeles Harbor is basically anticyclonic with the outfall waste being rapidly discharged into the Strait of Juan de Fuca, the data indicate diverse eddy and turbulent motion at all depths. This motion would be expected to carry wastes into the Harbor.

The drogue* studies were generally synoptic in that several drogues were released at different points simultaneously. They were not synoptic with depth since all drogues were set at 4 m (13 ft) after earlier trials indicated this represented the upper 8 m (26 ft) of the water column. There were distinct changes in water transport direction within relatively small distances, indicating eddy and turbulent motion.

For example, in the mid-ebb release for 22 July 1970 [Fig. III-7], drogue Nos. 4, 7, 8, 10, 13 and 14 moved from the mouth of Port Angeles Harbor east to the vicinity of Morse Creek. However, drogue Nos. 9 and 11, only a few hundred meters northeast, moved in the opposite direction, north and then west around Ediz Hook. Figures III-8 and 9 provide additional examples. Six releases, at mid-flow, low slack, late ebb to low slack, mid-ebb, and high slack tide, all show definite rotary movement. Figure III-10 shows the low slack release. On one occasion, the

* Drogue assembly is shown in Fig. IV-2.

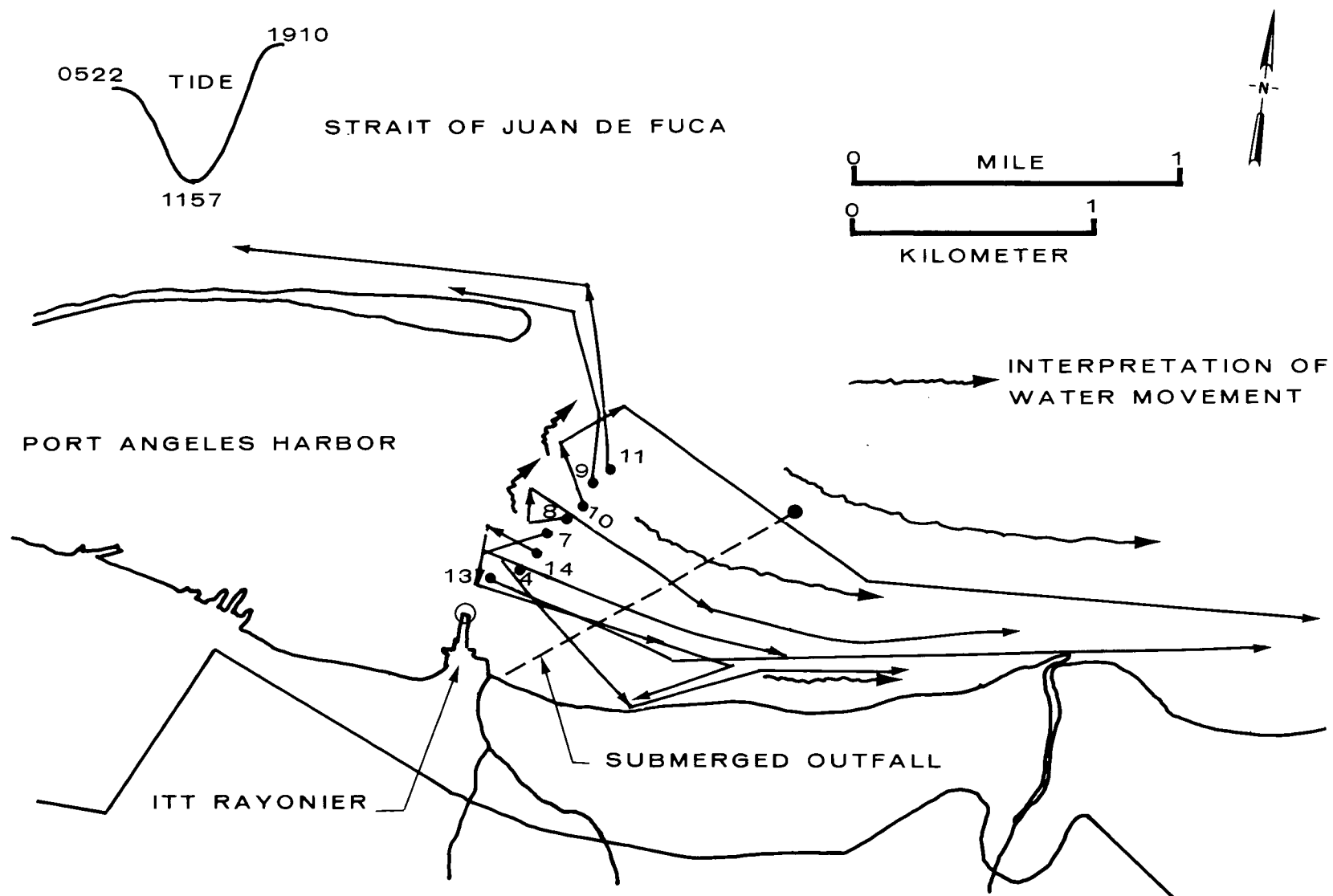


Figure III-7. Mid-Ebb Drogue Release (ITT Rayonier, 7/22/70 2/)

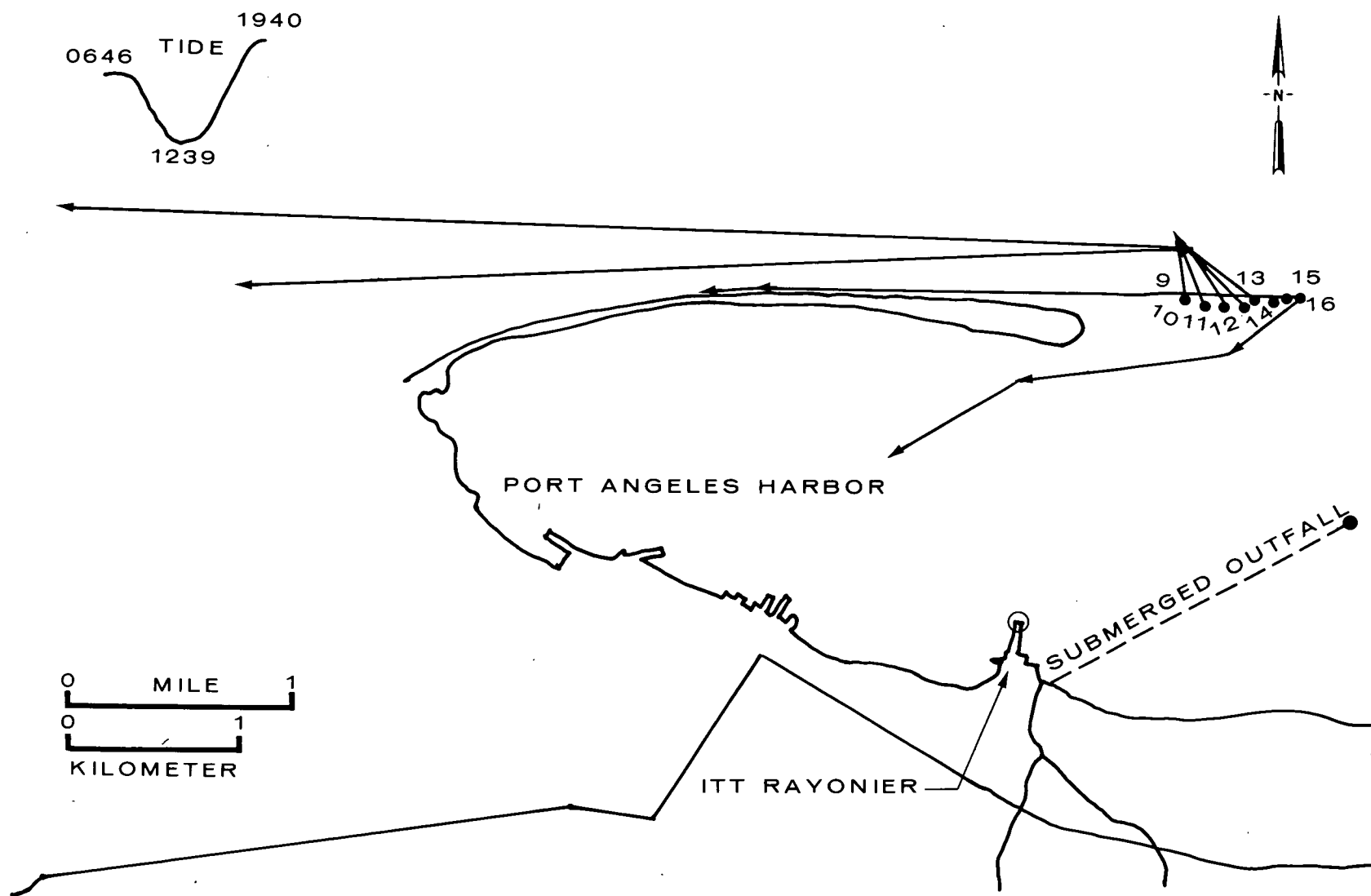


Figure III-8. Mid-Ebb Drogue Release (ITT Rayonier, 7/23/70 2/)

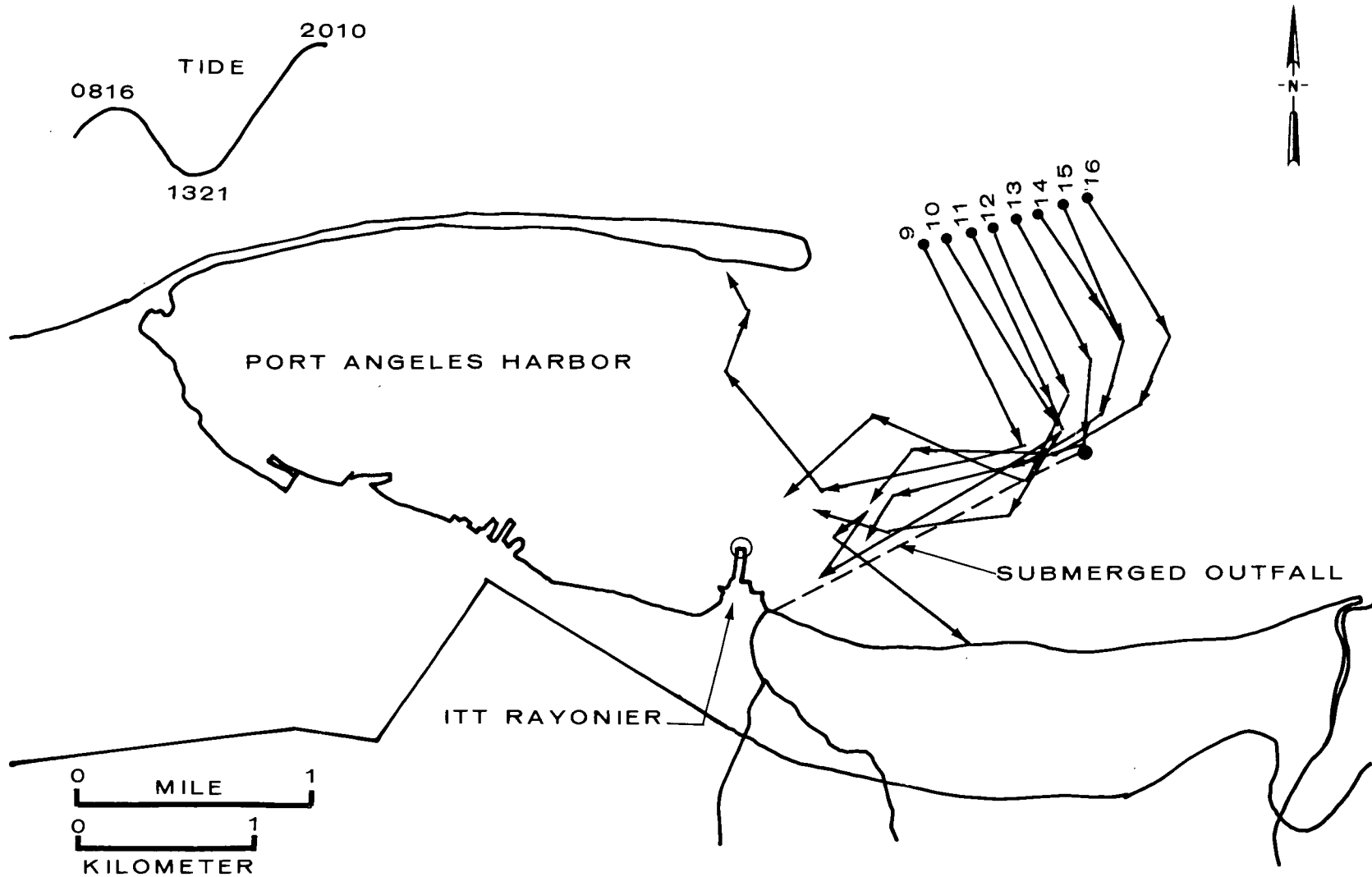


Figure III-9. High Slack Drogue Release (ITT Rayonier, 7/24/70 2/)

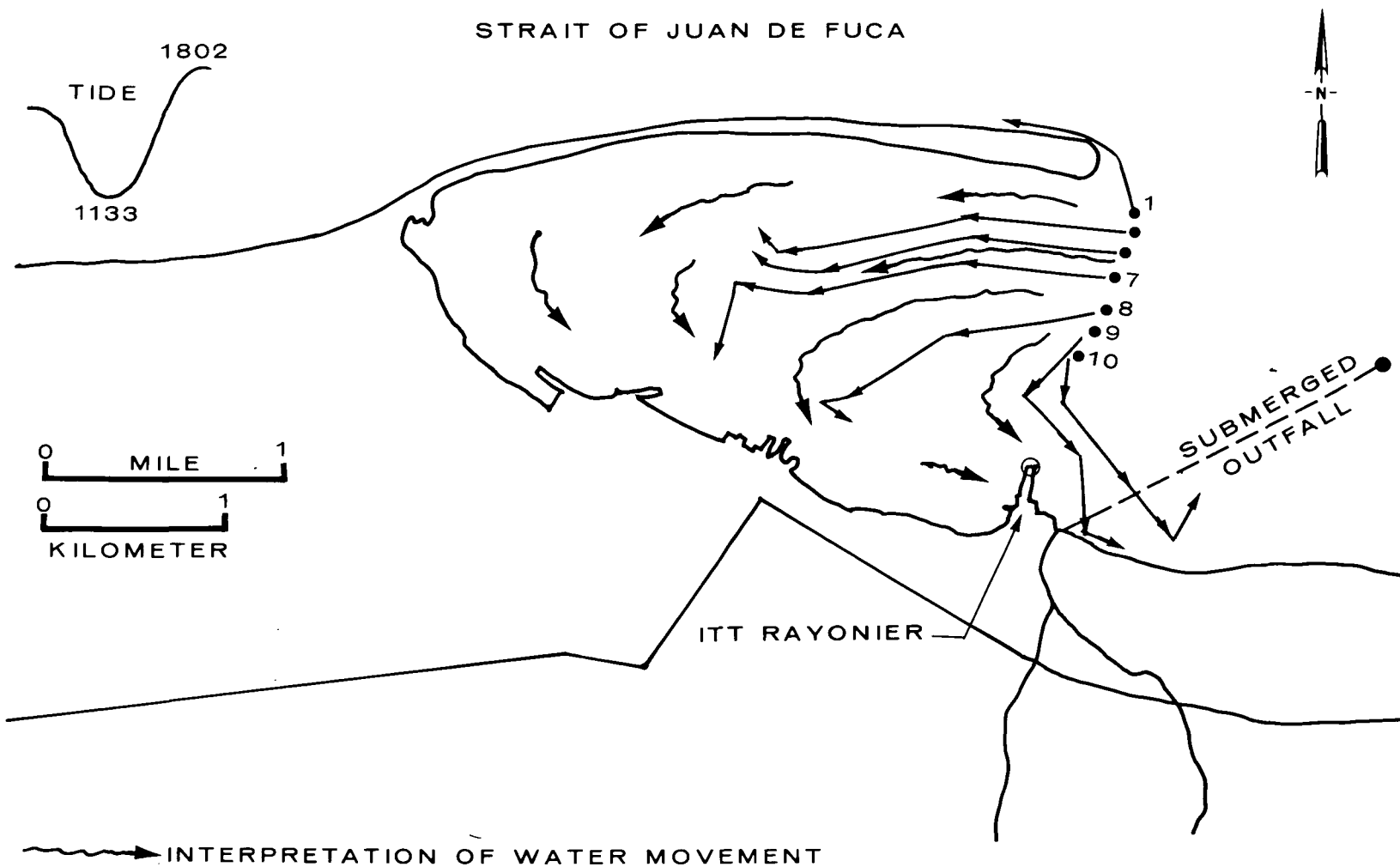


Figure III-10. Low Slack Drogue Release (ITT Rayonier, 8/20/70²)

midflood release for 28 July 1970, essentially linear motion was observed from the positions of drogue release. This infrequent occurrence indicates that rotary motion is the dominant feature in the Harbor area.

These drogue studies do not support the report's conclusion that the water motion is predominantly anticyclonic.

NATIONAL OCEANOGRAPHIC DATA CENTER (NORDAC)

To resolve discrepancies between the two reports, additional data were sought from the files of NORDAC. Of more than one hundred oceanographic stations surveyed in the Strait of Juan de Fuca from 1930 to present, twenty were selected as being sufficiently close to Port Angeles Harbor to be useful. The closest station lies about 3 km (2 mi) north of the point of Ediz Hook. The others lie further to the north and northwest [Fig. III-11].

Water Density and Temperature

The data of interest for these stations are the variation in σ_T with depth, and the decrease of dissolved oxygen with depth. The parameter σ_T is defined as

$$\sigma_T = 1000 (\rho - 1.0) \quad (1)$$

where ρ is the water density in gm/cc. The σ_T values assume one atmosphere of pressure at the sea surface.

Salinity is derived from a determination of the chlorinity of sea water by the empirical formula:

● 14. (10/7/57) ● 2. (27/01/54)

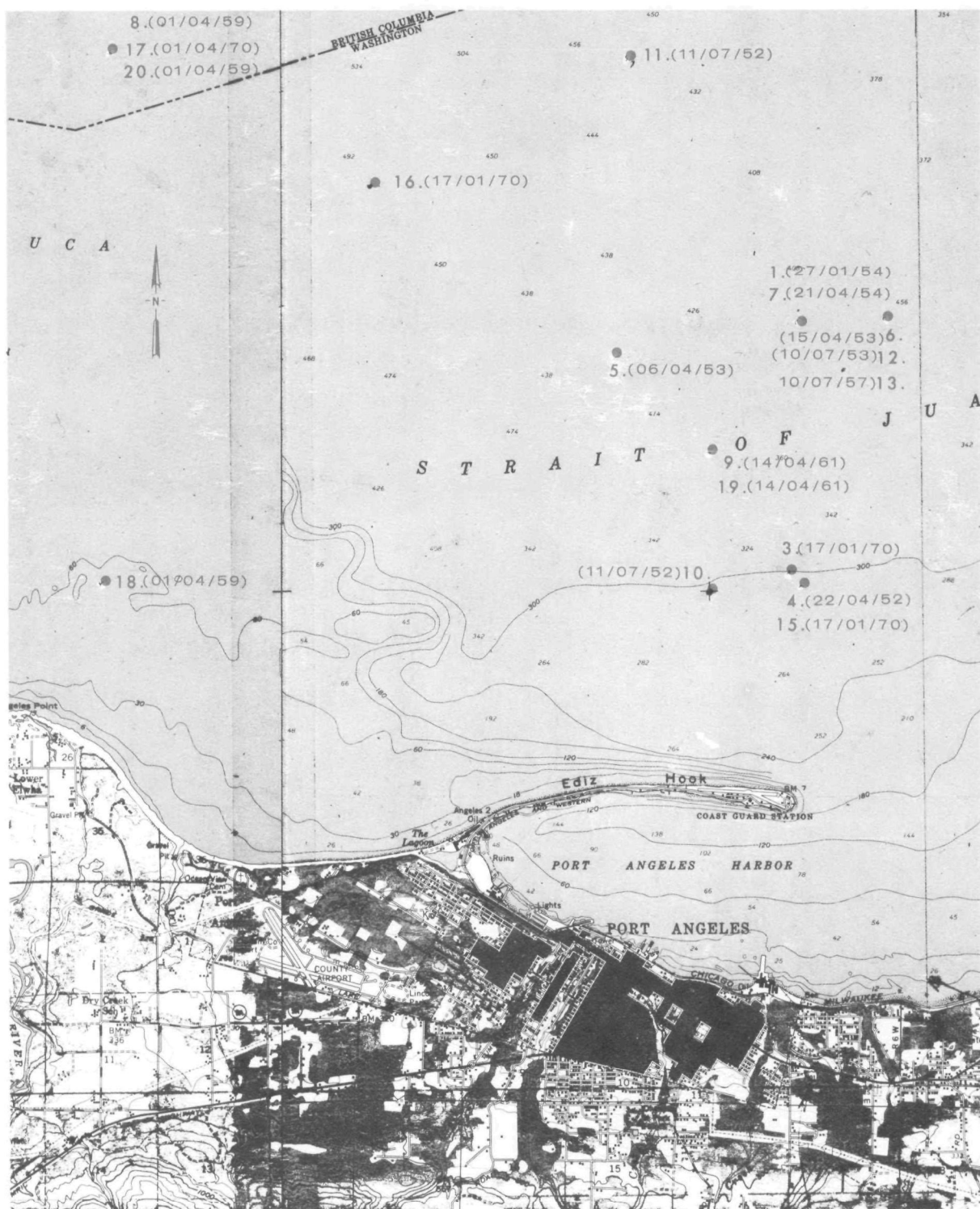


Figure III-11. Oceanographic Stations
in the Strait of Juan de Fuca

$$S \text{ o/oo} = 0.03 + 1.805 \text{ Cl o/oo} \quad (2)$$

where: $S \text{ o/oo}$ = salinity (parts per thousand)

Cl o/oo = chlorinity (parts per thousand of halogen concentration)

Density or σ_T at 0°C is obtained from salinity by the formula:

$$\sigma_T = -0.093 + 0.8149S - 0.000482S^2 + 0.0000068S^3 \quad (3)$$

The measurements necessary for determining these parameters have been standardized for several decades.

The depth of the ITT Rayonier outfall diffuser ranges from 17.1 m (56 ft) to 19.8 m (65 ft). Any sudden changes in either σ_T or dissolved oxygen to a depth of about 20 m (66 ft) would be indicative of the formation of a thermocline or pycnocline and a non-homogeneous water mass to a depth of the outfall. However, only indications of homogeneous mixing of water masses with a gradual increase in density with depth were observed. In fact, at Stations 4, 5 and 11 the density decreased at depth, indicating strong dynamic motion in the surface layers.

Stations 15 through 20 are bathythermograph stations showing the change in temperature with water depth. Any sudden change in temperature decrease with depth would have been indicative of thermocline development, but none was found. Although no stations were sampled during autumn, which would be the most likely time for thermoclines

to develop, their presence seems unlikely since no tendency towards thermocline development was noted during the winter, spring or summer. The data indicate that the water is reasonably homogeneous throughout the year, at least to 18 m (60 ft), the approximate depth of the ITT Rayonier outfall.

STORET DATA*

Bioassay studies with juvenile salmon indicated that to protect young salmon and other fishes the spent sulfite waste liquor concentrations (measured by the Pearl-Benson Index) should be less than 1,000 ppm at all times and at all locations in Port Angeles Harbor.

Storet data for Port Angeles Harbor indicates that at only one station, adjacent to the outfall, was spent sulfite liquor measured since the outfall went into operation in September 1972. This station is 200 m (650 ft) due west of the southernmost diffuser port on the outfall. For the week beginning 31 October 1972 the mean value of six samples was 14,750 ppm of spent sulfite liquor, according to the Pearl-Benson Index, with a maximum of 18,800 ppm and a minimum of 7,600 ppm.

The ITT Rayonier report anticipated the concentration at this station to be less than 300 ppm under the worst possible conditions when the current is moving directly west across the outfall [Figure III-12].

*STORET is an EPA water quality data base.

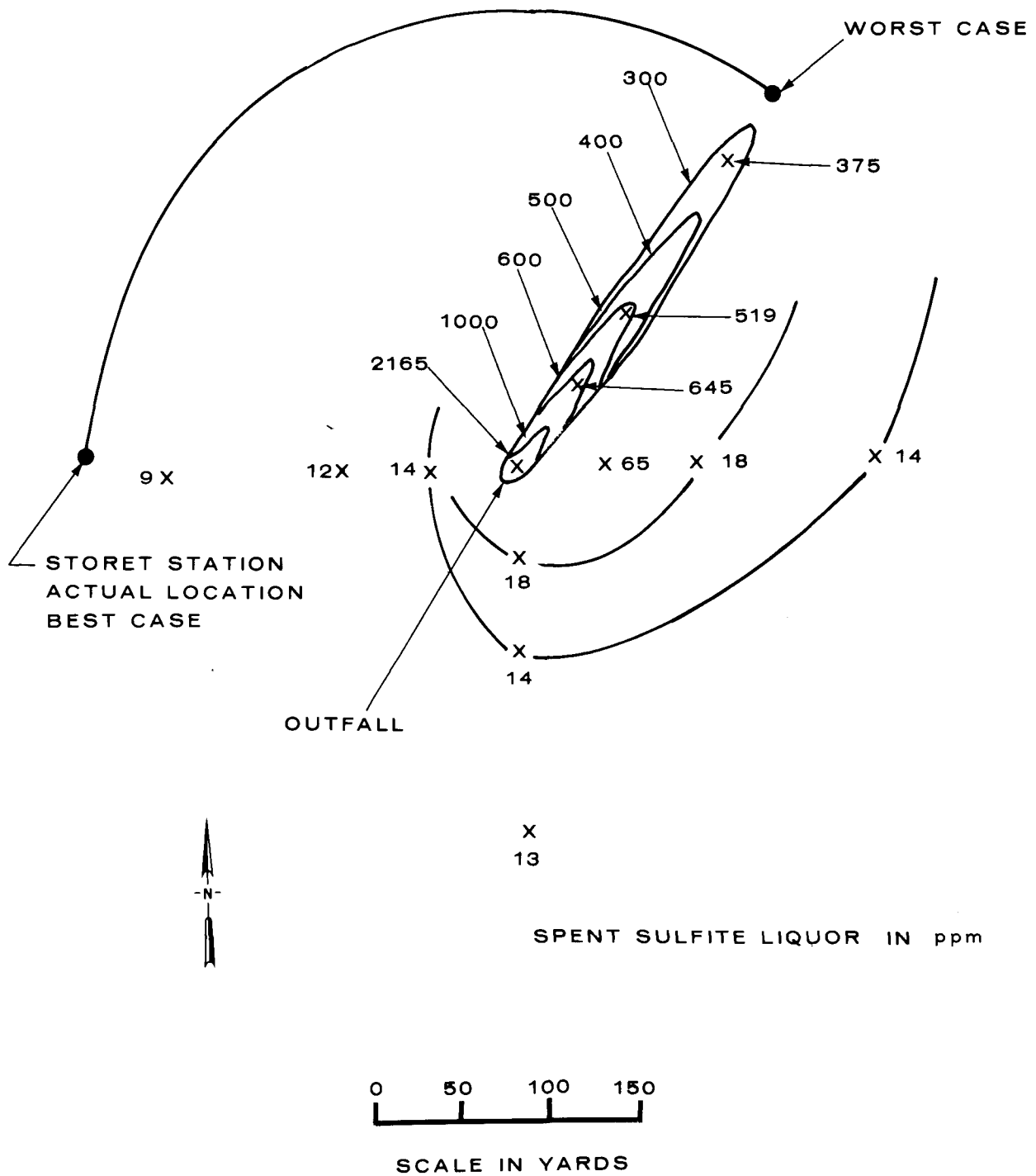


Figure III-12. Predicted Discharge Characteristics
of the Outfall for the Spent Sulfite Liquor 2

Thus on six consecutive days spent sulfite liquor concentrations ranged from 25 to 60 times greater than the predicted level. The ITT Rayonier report indicates that heavy foam generation begins to occur when the spent sulfite liquor concentration exceeds 80 ppm. Therefore, foam could be expected in this case even though the study concluded that as a result of the outfall none would occur.

IV. REMOTE SENSING STUDY

The remote sensing study was conducted on 24-25 April and 25 July 1973. It included drogue studies and the analysis of physical and chemical properties of Port Angeles Harbor.

The times of flight over Port Angeles Harbor were predicated upon the tide levels or phases in the immediate area [Table IV-1]. The duration of flight ranged from 1 to 1½ hr [general procedures in App. A].

Table IV-1
Tide Phase Data At Port Angeles

Date (1973)	Time	Water Height Above Mean Sea Level		Tide Phase ^{a/}
		(m)	(ft)	
	<u>PST^{b/}</u>			
24 April	0115	1.7	5.5	HLT
	0256	1.7	5.6	LHT
	1304	0.1	0.3	LLT
	2142	2.0	6.6	HHT
25 April	1359	0.2	0.7	LLT
	<u>PDT^{c/}</u>			
25 July	0521	-0.3	-1.0	LLT
	1355	1.8	6.0	LHT
	1638	1.7	5.6	HLT
	2212	2.2	7.3	HHT

^{a/} Tide Phases: L = Low; H = High; T = Tide
^{b/} Pacific Standard Time
^{c/} Pacific Daylight Time

Figure IV-1 shows the relationship between the times of flight and the tide phases (LLT - low low tide, HLT - high low tide, LHT - low high tide, HHT - high high tide). The first flight in April was flown near the end of the LHT-LLT phase, the second near the end of the LLT-HHT phase, while the third was carried out early in the HHT-LLT transition. These tide/time phase conditions represented a weak dynamic state in the Harbor waters providing minimal mixing between the ITT Rayonier diffuser effluent and the receiving water. In July the two flights were carried out in a nearly slack tide condition, also indicative of minimal mixing.

DROGUE (CURRENT) STUDY

The drogue assembly consists of three integral units: the drogue unit, depth line, and surface float [Fig. IV-2]. The four drogue assemblies deployed for each flight were adjusted by the depth line to 0 m (surface), 3 m (10 ft), 6 m (20 ft), and 12 m (40 ft) depths. They were carried to the diffuser and released next to a 1.22 x 4.88 m (4 x 16 ft) panel that had been tied with line and anchored to the ITT Rayonier diffuser for a reference point.

The movement of the drogues, caused by the current at the depth of the drogue unit, was monitored photographically by an aircraft for at least an hour. During the nighttime missions, gas lanterns were mounted on the surface floats to serve as heat targets which were monitored by the infrared line scanner in the aircraft.

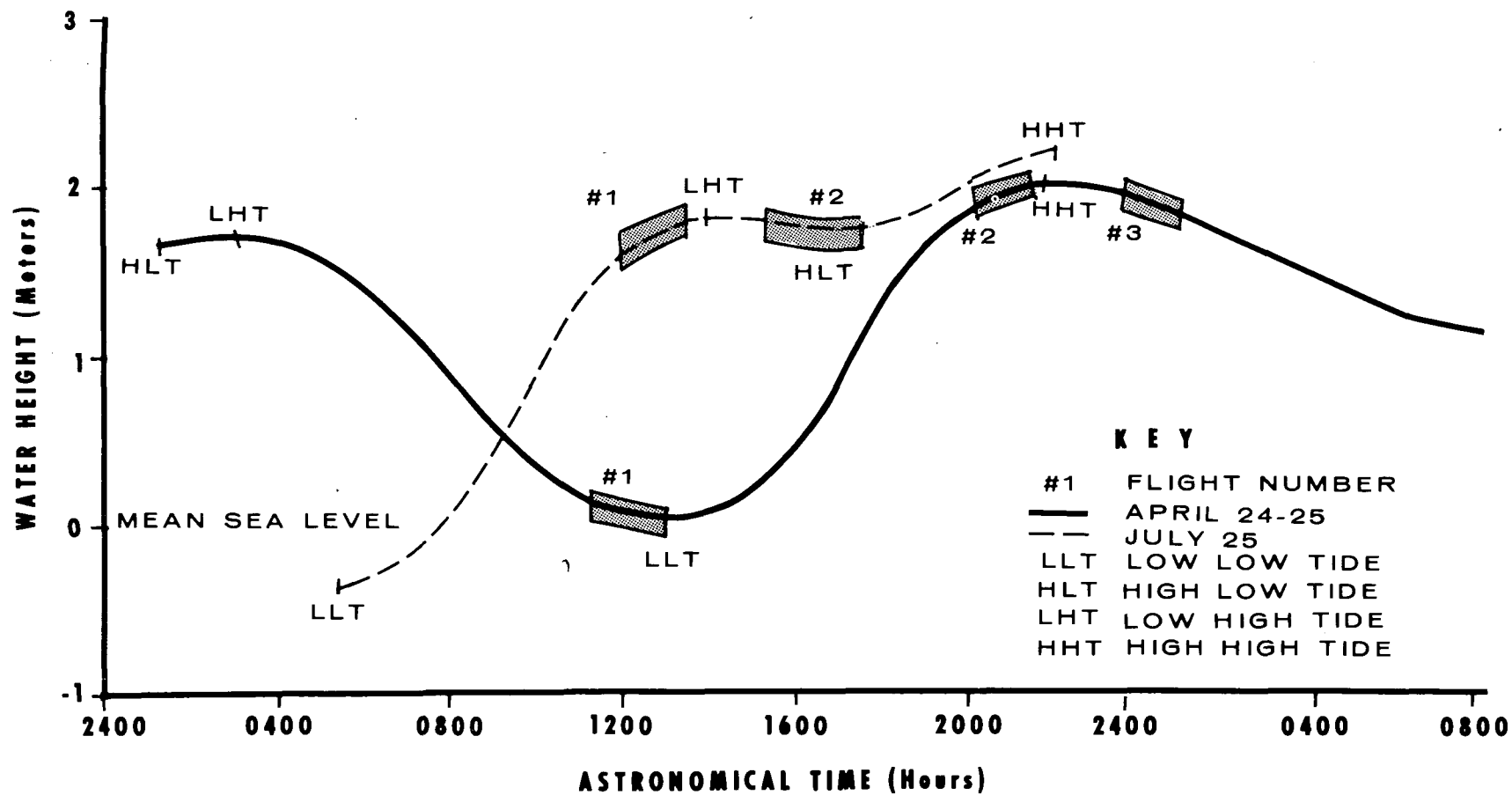


Figure IV-1. Tide Conditions and Duration of Flights

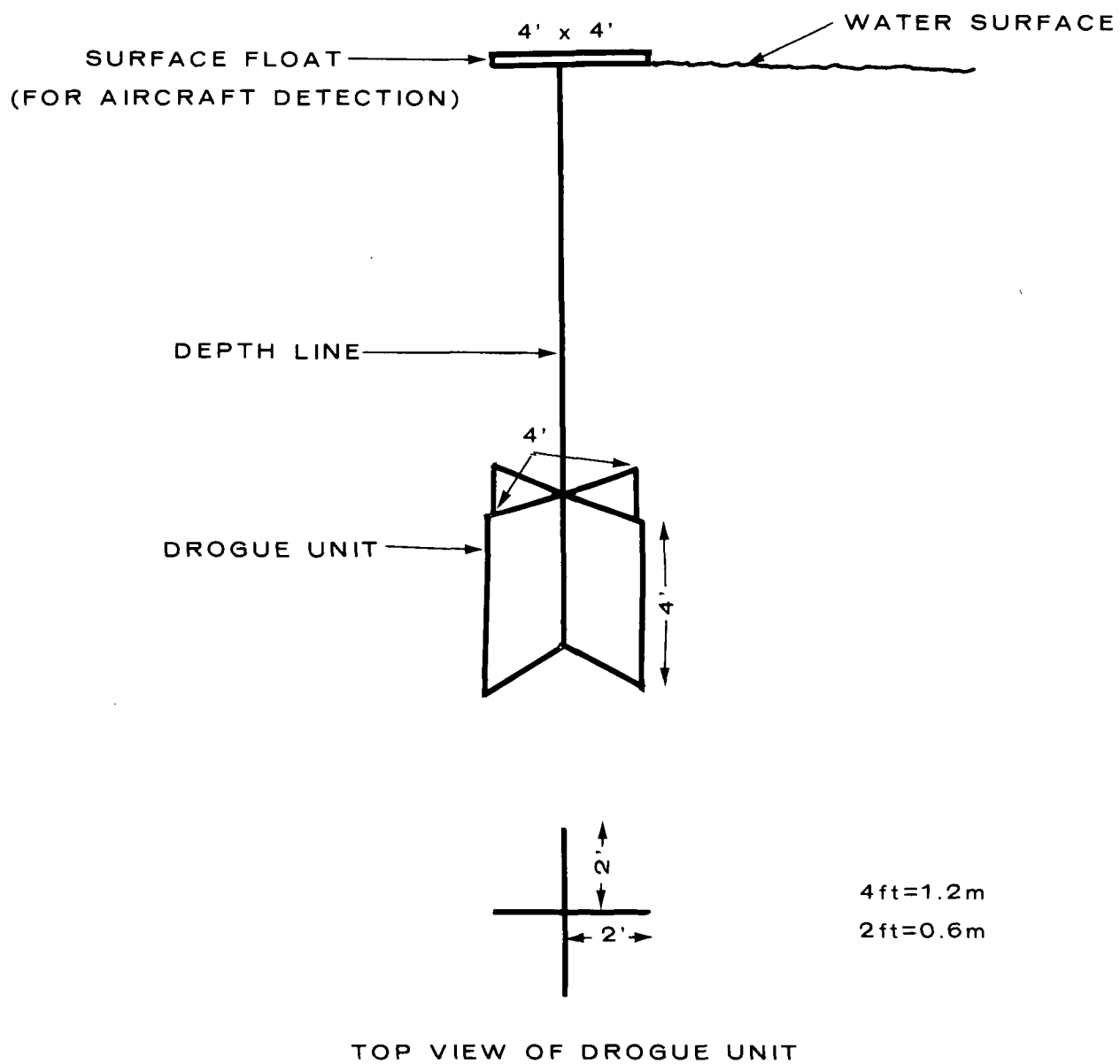


Figure IV-2. Drogue Assembly

WATER QUALITY DATA (GROUND TRUTH)

Water quality data were collected from twelve discrete points in Port Angeles Harbor during the daylight flights [Fig. IV-3]. The data included:

1. Water surface temperature
2. Dissolved oxygen (DO)
3. pH
4. Conductivity
5. Turbidity
6. Total suspended solids (TSS)
7. Total suspended solids, non-volatile
8. Pearl-Benson Index (PBI) for spent sulfite liquor

The values for the above parameters, obtained during the April flights, are provided in Table IV-2.

Only water surface temperatures were measured by ground personnel during the night missions because the only sensor used during that phase of the program was the infrared (thermal) line scanner.

In addition to the above data, a sample of the diffuser effluent was collected from the ITT Rayonier plant. The effluent was spectroscopically tested to characterize its unique optical properties, or "fingerprint." The fingerprint was the criterion for analyzing the airborne imagery.

Weather information was an important requirement of the sampling program, especially wind vector data for tracing surface and near-surface currents in the Harbor. The weather conditions, recorded at the U. S. Coast Guard Air Station at the east end of Ediz Hook [Fig. IV-3] at the time of each flight, are provided in Table IV-3.

Figure IV-3. Water Quality Data Stations
(Station Number Encircled; Dot Depicts Location)

Table IV-2

Ground Truth Data for Port Angeles Harbor
[24 April 1973, 1130 to 1250 hours PST]

Station ^{a/}	Hour	Surface Temperature (°C) (°F)		DO ^{b/} (mg/l)	pH	Conduc- tivity (μmho/cm)	Turbidity (JTU)	TSS (mg/l)	TSS [non-vol] (mg/l)	PBI ^{c/}
1	1240	11.3	52.3	9.1	7.8	46,500	0.6	14	4	10
2	1300	12.1	53.8	9.0	7.5	44,500	2.8	23	4	200
3	1315	11.5	52.7	9.1	7.8	45,500	0.7	18	5	5
4	1345	11.1	52.0	9.2	7.8	45,500	1.3	19	3	6
5	1230	8.0	46.4	9.4	7.5	45,500	2.2	19	6	30
6	1240	8.5	47.3	9.2	7.8	46,500	1.0	18	7	15
7	1245	9.0	48.2	9.0	7.7	43,500	1.1	21	9	19
8	1250	10.0	50.0	9.2	7.9	45,500	1.4	23	10	20
8	1255	10.5	50.9	9.2	7.8	46,500	0.6	20	7	11
9	1303	12.5	54.5	9.9	7.9	46,500	0.6	20	6	17
10	1310	13.0	55.4	9.2	7.9	26,800	0.6	19	6	3
11	1315	21.0	69.8	---	2.5	16,200	1.8	31	6	233,000
12	1320	12.0	53.6	9.3	7.8	46,500	0.4	15	4	7

^{a/} Depth of Station 8 at 1255 hr was 3 m (10 ft); depth of all other stations was 0 m.

^{b/} Measurements collected by a hydrolab ionic probe.

^{c/} Pearl-Benson Index: concentration of lignin in water (mg/l) from natural sources and pulp/paper mill effluents.

Table IV-3
Meteorological Data

Date (1973)	Flight	Air Temperature (°F)	Wind		Sky
			Direction (°)	Speed (kn)	
24 April	1	52	030	3	Clear
	2	51	030	5	Clear
	3	47	250	3	Clear
25 July	1	66	060	1	Clear
	2	67		Calm	Clear

RESULTS OF DROGUE STUDY

As mentioned above, there were three flights during the drogue study on 24 April and two on 25 July. The results from these five flights are presented as time-distance tables [App. B] and vector diagrams, where practicable.

The first flight on 24 April was flown 1137 to 1350 hours Pacific Standard Time during an ebb tide [Fig. IV-1]. The four drogues were released near the reference panel which was anchored to the ITT Rayonier diffuser. Table B-1 contains data for the motion of each drogue. These data have also been plotted as polar coordinates in Figure IV-4; each segmented line represents the movement of a particular drogue assembly. The surface and 3 m (10 ft) drogues moved in similar paths. The 6 m (20 ft) drogue hooked more quickly than the more shallow drogues. The 12 m (40 ft) drogue hooked quite sharply in the cyclonic direction propagating no more than 150 m (490 ft) radially from the reference panel. This shows that a moderate vector change in current magnitude and

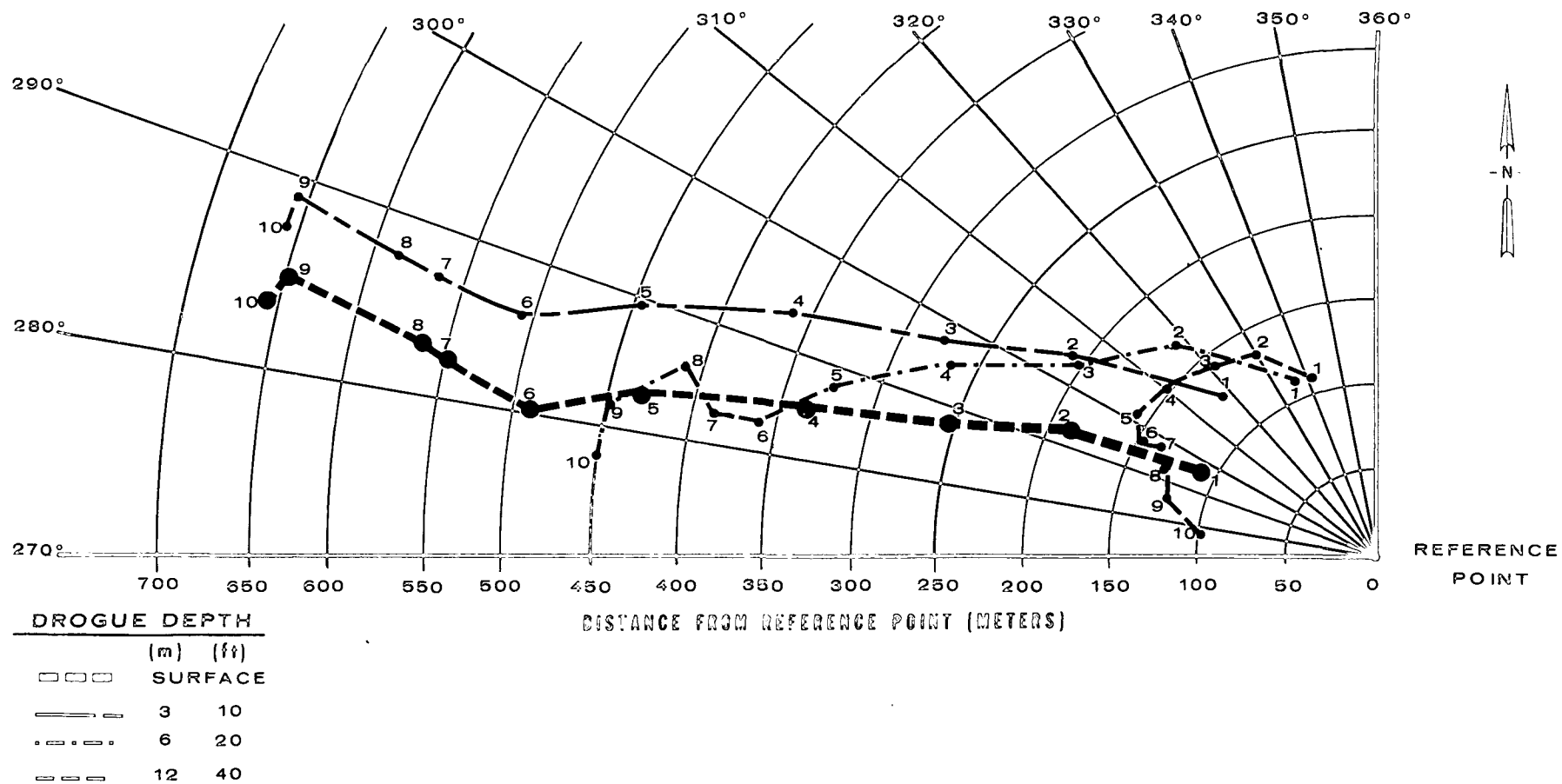
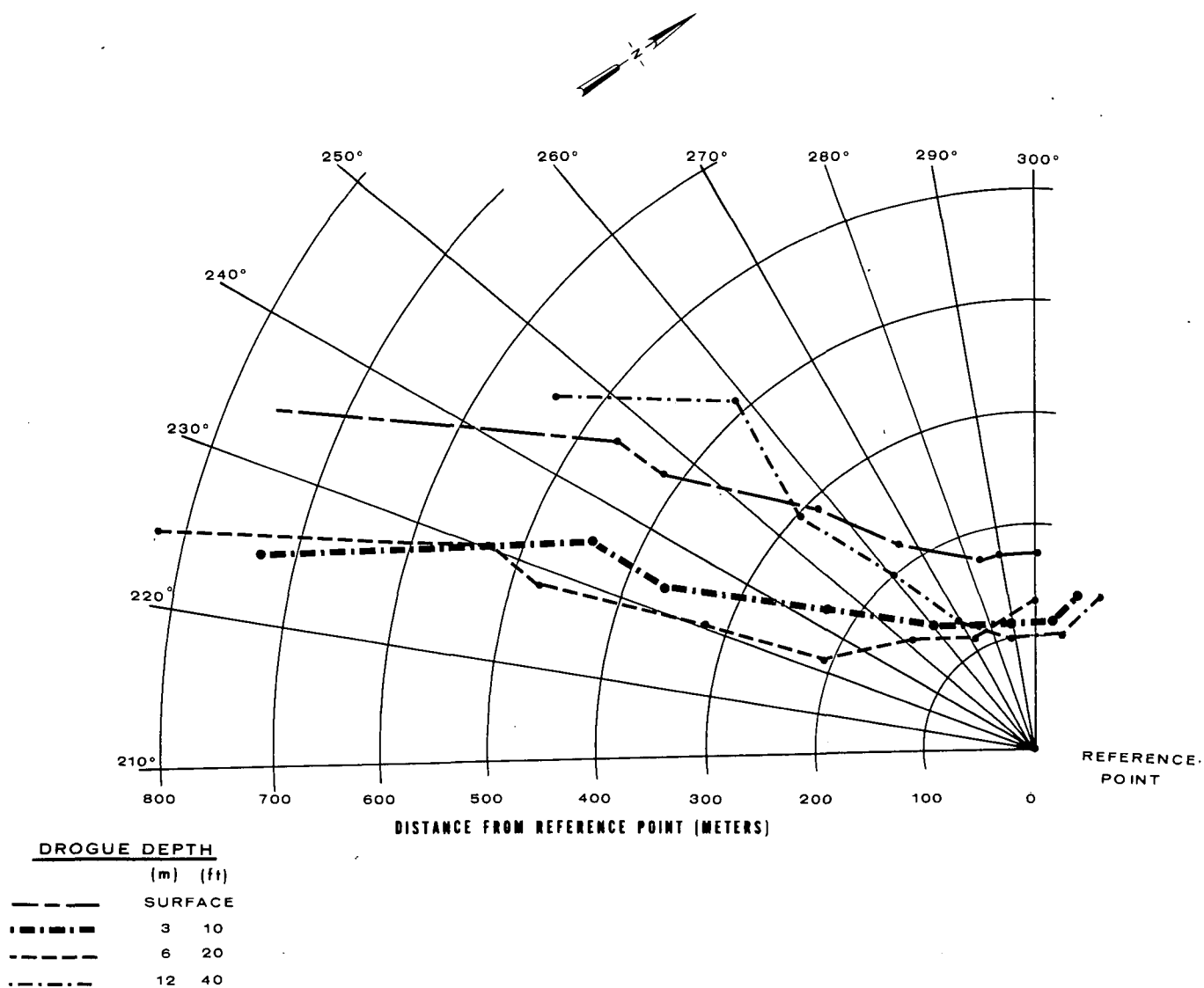


Figure IV-4. Drogue Vector Diagram, Flight #1 (NFIC-D, 4/24/73)

direction took place between the 3 m (10 ft) and 6 m (20 ft) depth, and a greater change occurred between 6 m (20 ft) and 12 m (40 ft). Thus the effluent dispersed from the diffuser to 12 m (40 ft) deep will probably have higher concentrations than at levels closer to the surface. The effluent which dispersed to between the surface and 3 m (10 ft) would propagate a significant distance into the Harbor before dispersing. During this flight the diffuser plume did reach the surface and move in a westerly direction. Visual discoloration was traced approximately 1.5 km (0.9 mi) west of the reference panel before disappearing.

The tabulated data for the second flight are given in Table B-2 and the vector diagram derived from these data in Figure IV-5. This flight was made during slack high water [Fig. IV-1]. All the drogues moved southwesterly, and the 6 m (20 ft) drogue was furthest displaced. The drogues displayed no cyclonic displacement as during the first flight, with the possible exception of the 12 m (40 ft) drogue. However, during the latter portion of the flight it rotated into a line of propagation nearly equal in polar angle to the other drogues. These observations indicated that the effluent from the submerged diffuser could be carried by the tidal currents into the Harbor without evidence of a cyclonic spin-off to the Strait of Juan de Fuca. No visible plume was recorded because this was a night flight and the Infrared Line Scanner (IRLS) was the only active sensor.

Data for the last flight in April which was conducted on an ebbing tide, are tabulated in Table B-3. The vector diagram [Fig. IV-6]



**Figure IV-5. Drogue Vector Diagram, Flight #2
(NFIC-D, 4/24/73)**

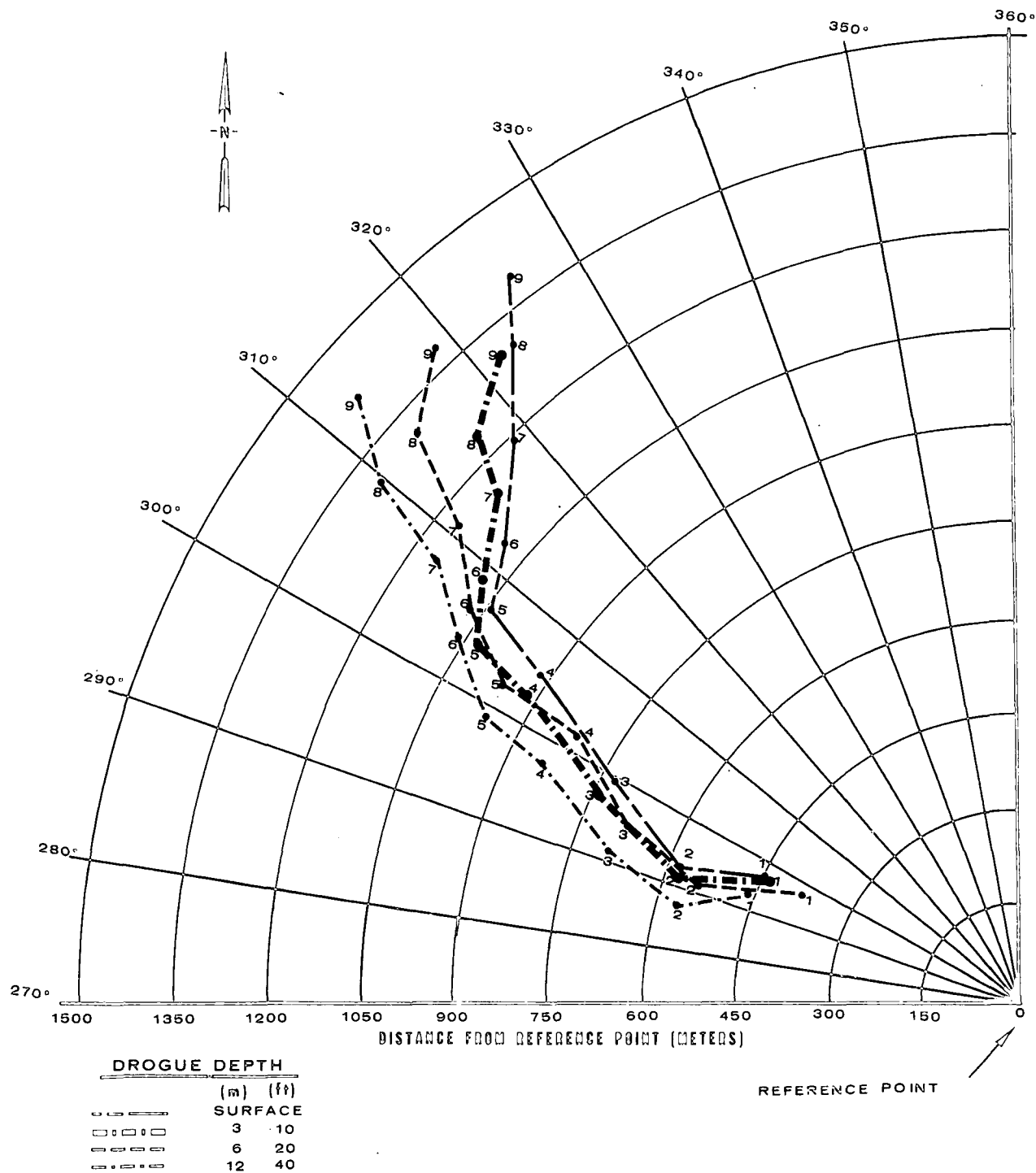


Figure IV-6. Drogue Vector Diagram, Flight #3
(NFIC-D, 4/24-25/73)

shows that the four drogues initially traveled in a westerly direction (271° true) before abruptly changing direction (average heading of 314° true) toward the Strait of Juan de Fuca. About 45 min after release, the drogues were traveling north and were east of Ediz Hook [Fig. IV-3]. The effluent was being carried directly to the Strait; it did not enter and disperse in Port Angeles Harbor.

Two daylight flights were conducted on 25 July near slack tide [Fig. IV-1]. Some difficulty was encountered in monitoring the surface panels on the drogues because of the quiescent meteorological conditions and heavy ship traffic in the Harbor. The surface waters acted like a mirror to reflect the clouds and sky above the aircraft and mask the drogues' surface floats. Thus the July data are not as complete as the April data.

During these flights the drogues were positioned at 1.6 m (5 ft), 4.6 m (15 ft), 6.1 m (20 ft) and 12.2 m (40 ft) depths at the request of EPA Region X. There was no surface drogue.

The first flight was from 1207 to 1307 hours Pacific Daylight Time during rising tide [Fig. IV-1]. The 12.2 m (40 ft) drogue was observed only twice, traveling west-southwest with respect to the reference point [Fig. IV-7]. Midway through the flight two neighboring drogues could not be distinguished from each other; their depths were unknown. On the sixth pass one of the drogues was traveling with a heading of 243° , while on the ninth pass the same or another drogue was traveling due west. The fourth drogue was not observed.

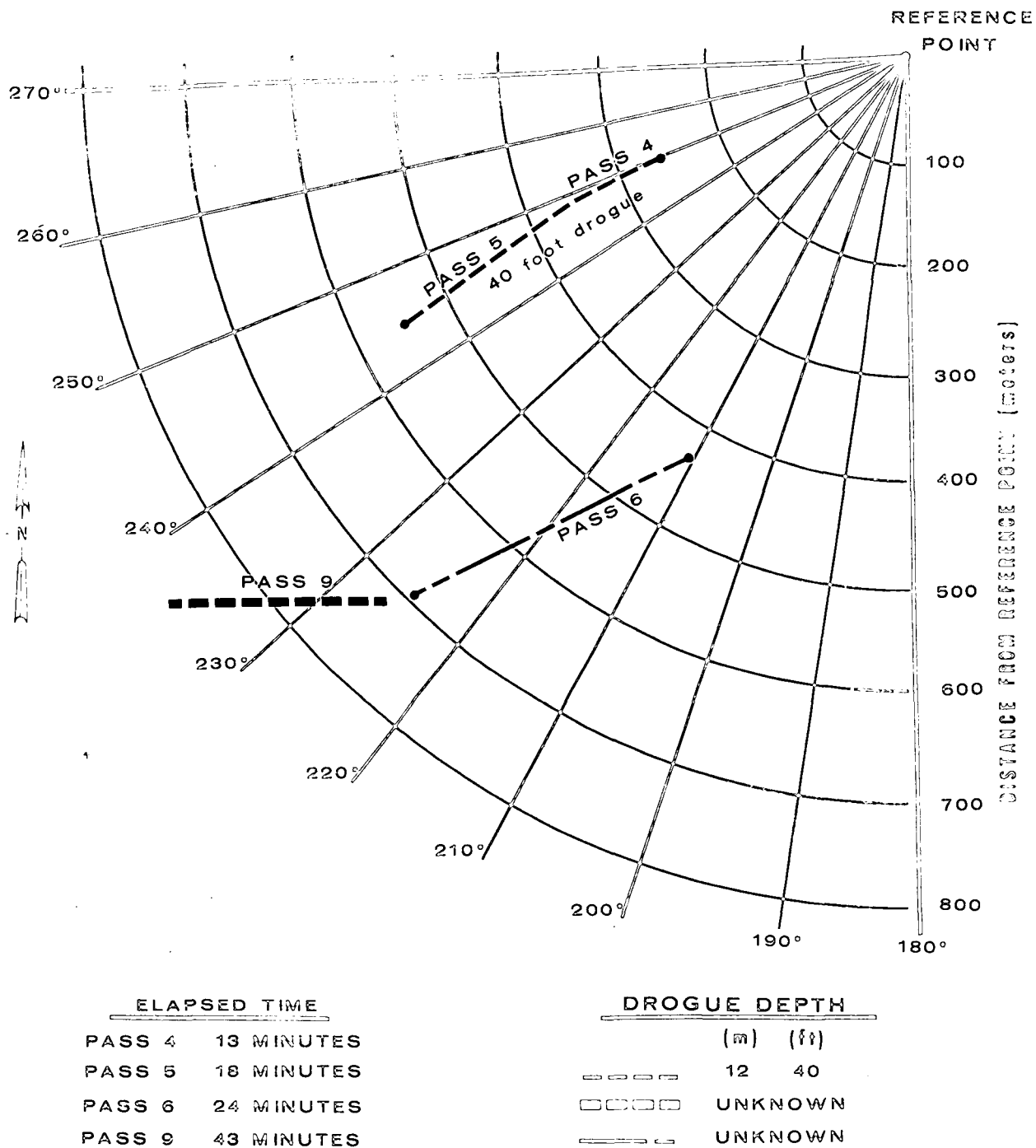


**Figure IV-7. Drogue Vector Diagram, Flight #1
(NFIC-D, 7/25/73)**

The final flight was from 1530 to 1630 hours PDT during a slack tide [Fig. IV-1]. Only the last pass recorded both the reference panel and three of the four drogues. The 4.5 m (15 ft) drogue was not sighted. Figure IV-8 shows a single dashed line representing the reference point and the only position of the remaining three drogues. The line's heading is 318° . In 1 hr the drogues had moved 1,500 m (5,000 ft) from the reference panel. Had they continued along the average heading, they would have passed within 215 m (705 ft) of Ediz Hook in approximately 31 min. The tide phase at that time remained for an additional $4\frac{1}{2}$ hr after the last pass. Barring the effects of any significant cyclonic currents, the effluent from the diffuser would have dispersed in the Strait.

ANALYSIS OF EFFLUENT CONCENTRATIONS

A major purpose of this study (Section I) was to determine optically if the diffuser effluent was dispersing within the established zone of dilution [Fig. IV-9] and, subsequently, if the temperature of the effluent was greater than 0.28°C (0.5°F) above ambient leaving the dilution zone en route to surface waters.

During the first flight on 24 April the plume from the diffuser was reaching the surface and dispersing along a heading of 260° (westerly) from the reference point anchored to the diffuser [Fig. IV-9]. The width of the plume as it surfaced was 290 m (995 ft); the measured distance between the panel and the plume was about 12 m (40 ft).

Thirteen frames (Fig. IV-10 represents the first frame of the sequence) of true-color imagery were analyzed for color characterization

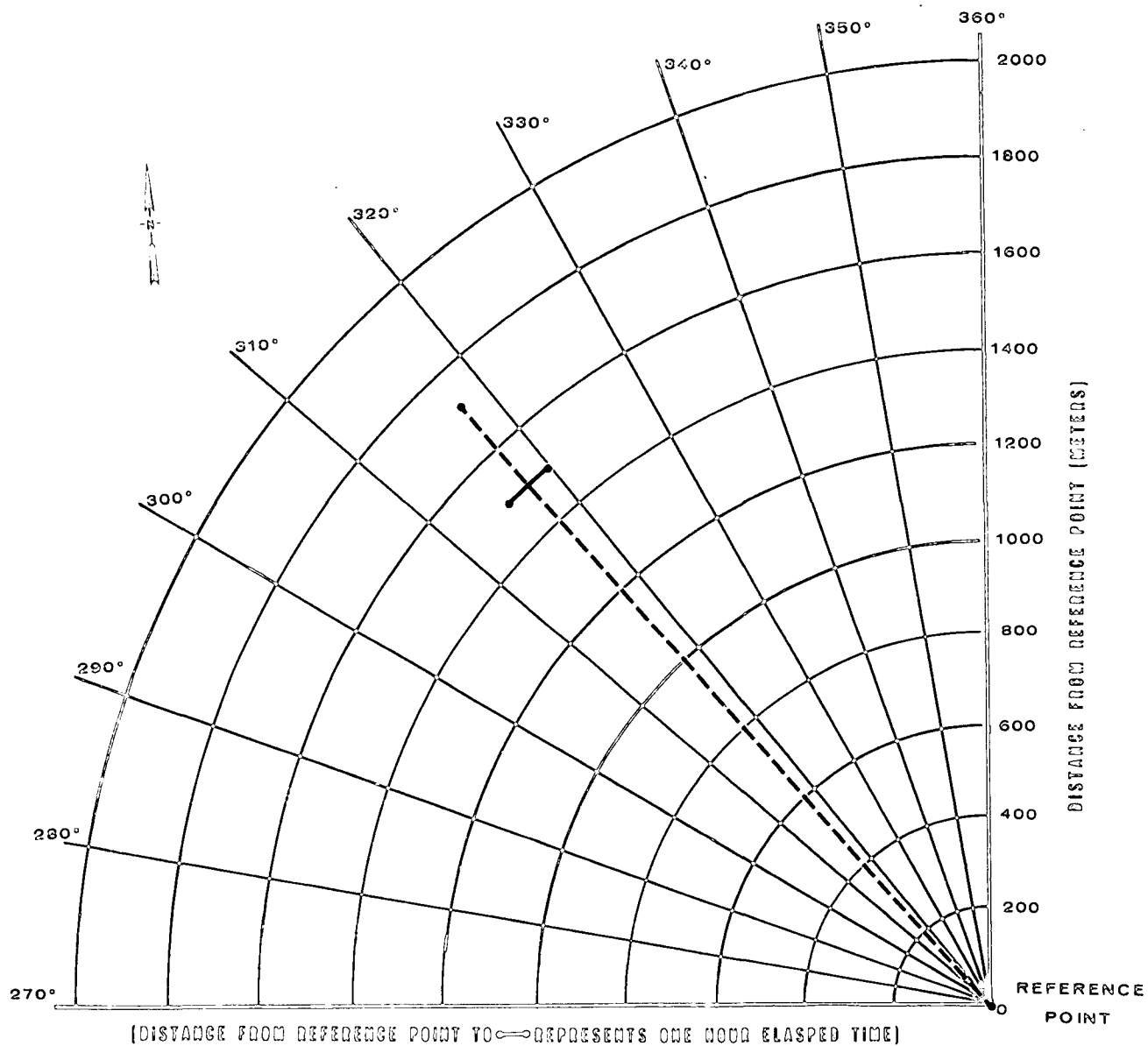


**Figure IV-8. Drogue Vector Diagram, Flight #2
(NFIC-D, 7/25/73)**

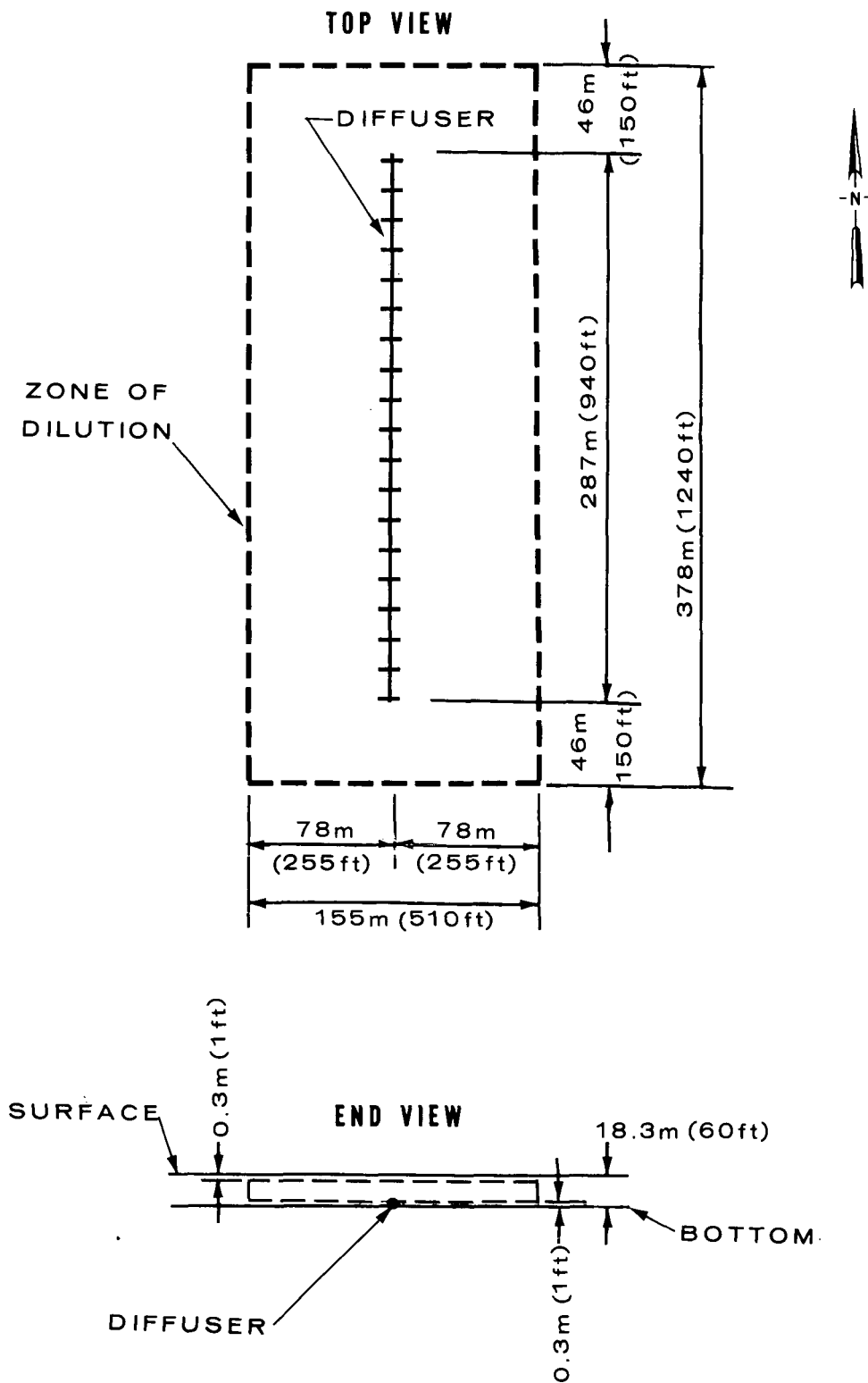


Figure IV-9. Zone of Dilution for the ITT Rayonier, Inc.
Submerged Diffuser

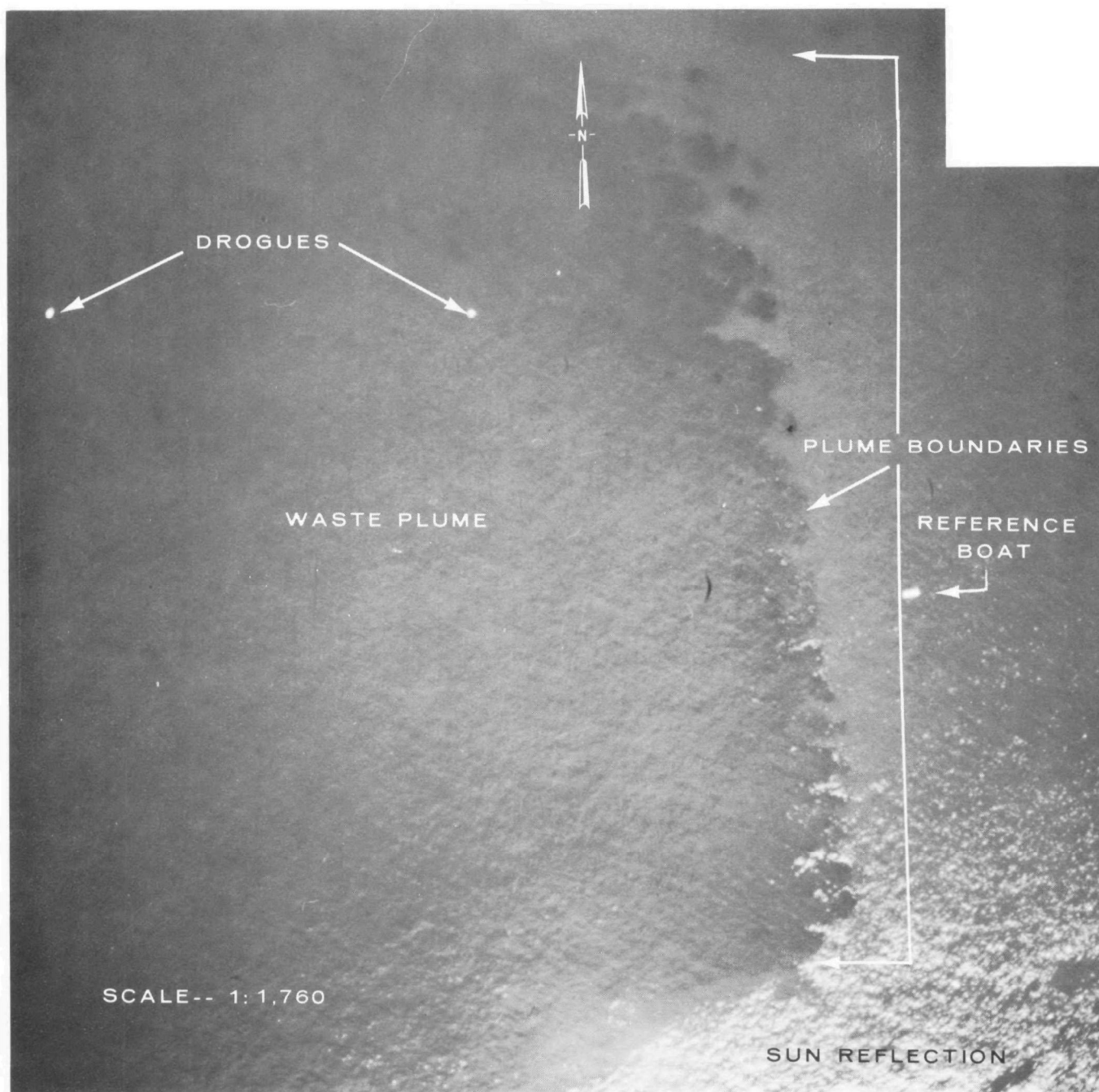


Figure IV-10. Plume from the ITT Rayonier Submerged Diffuser

from which isoconcentration lines throughout the plume were derived. In each frame, densitometer measurements [App. A] were made on a rectangular matrix with elements separated by 1 cm (0.4 in.). This spacing represents a 30 m (98 ft) interval at the water's surface. In the analyses the concept of optical linearity was assumed, in which there is a direct linear correlation between concentration and optical transmittance/scattering in the near-surface waters of the Harbor. Optically, the extinction depth* of the undiluted effluent was 4 cm (1.6 in.).

At the time of flight a liquid sample of the effluent to the diffuser was obtained from the ITT Rayonier facility. This sample was analyzed for its unique optical characteristics, or fingerprint. The sample was tested at 100, 50, 25 and 10 percent concentrations by dilution with background water, obtained at the time of flight from the Strait of Juan de Fuca near Ediz Hook. The optical data was subsequently used to analyze the film transmittance data obtained from the diffuser plume. The analysis indicated that the surface water just within the east (leading) edge of the plume [Fig. IV-10] contained a concentration of only 12 percent with respect to the undiluted effluent subjected to optical tests. For the remainder of the analysis, the area of highest concentration was normalized at 100 percent. An isoconcentration diagram [Fig. IV-11] was derived for 100, 50, 25, 10, and less than 10 percent concentration levels within the plume.

* Extinction depth is the maximum distance that red laser light can be transmitted through the effluent sample.

**PAGE NOT
AVAILABLE
DIGITALLY**

The perimeter of the dilution zone [Fig. IV-9] has been superimposed upon the isoconcentration diagram [Fig. IV-11]. The plume does not extend beyond the east zone boundary. However, the plume extends well beyond the west zone boundary and is detectable nearly 1.5 km (0.9 mi) west of the outfall. Because the length (longitudinal axis) of the zone was about 43 m (140 ft) greater than the angular coverage of the camera lens, the behavior of the plume at the south boundary of the dilution zone could not be determined.

The infrared (thermal) map recorded over the outfall [Fig. IV-12] shows that at the surface the plume was 0.5 to 1.0°C (0.9 to 1.8°F) cooler than the background surface waters of the Harbor. This indicates that there was no violation of the 0.28°C (0.5°F) upper temperature restriction at the boundary of the dilution zone.

Stereoscopic analysis of the photographic imagery shows that the effluent from the plume was passing through the 0.3 m (1 ft) upper boundary [Fig. IV-9] of the dilution zone to the surface, thereby not complying with the Washington State zone requirement. The thermal infrared data also confirm that the plume reached the surface of the receiving waters.

ITT RAYONIER DISCHARGES ALONG SHORE (Permit No. 071-06Y-2-038)

ITT Rayonier, Inc. has five outfalls which discharge along the southern shore of Port Angeles Harbor. These discharges have a combined flow rate of 1.5 m³/sec (34.5 mgd) and consist mostly of process and cooling water. They created a thermal plume of moderate size [Fig. IV-13] on 25 July. The plume dispersed easterly along shore. The

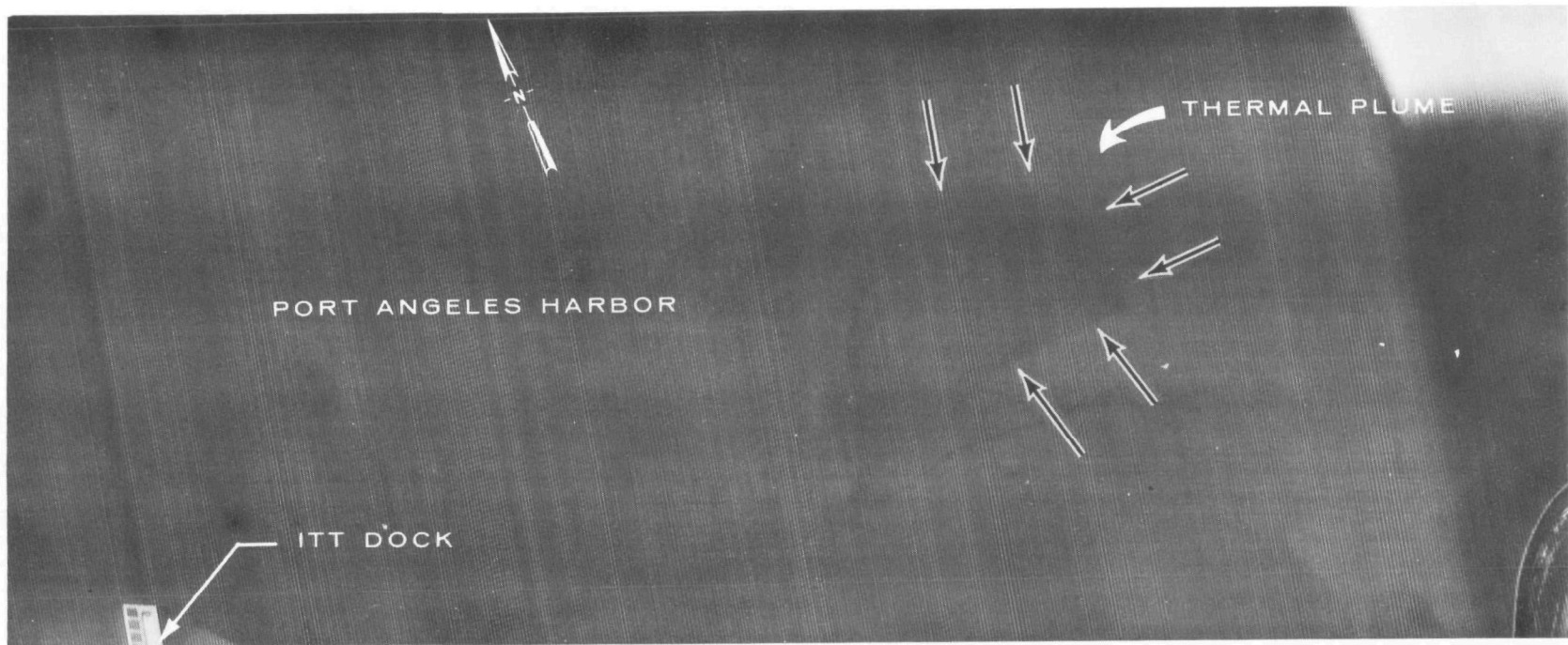


Figure IV-12. Thermal Infrared Map of ITT Rayonier Waste Plume from Submerged Diffuser

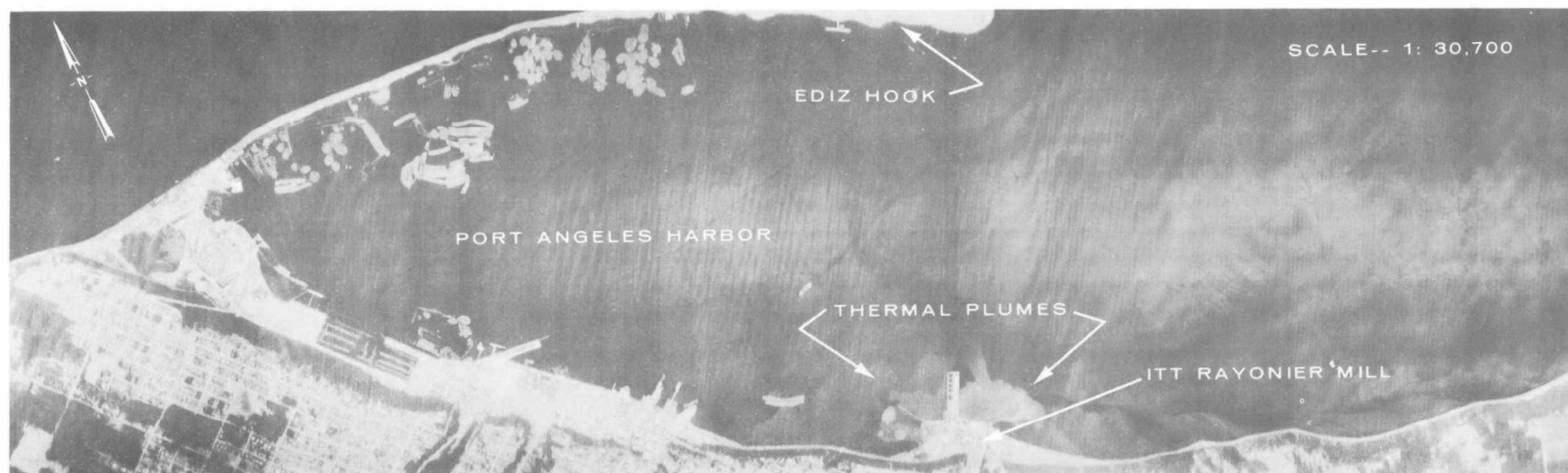


Figure IV-13. Thermal Infrared Map of Port Angeles Harbor and ITT Rayonier Discharges (7/25/73)

submerged discharge did not create a thermal plume at the Harbor surface during this flight.

CROWN ZELLERBACH CORPORATION (Permit No. 071-OYB-3-048)

Crown Zellerbach Corporation has eight active outfalls which originate at the mill site at the vertex of Port Angeles Harbor [Fig. IV-14]. Their points of discharge and average daily flow rates are as follows:

Table IV-4
Crown Zellerbach Corporation Flow Data

Outfall No.	Point of Discharge	Average Flow Rate	
		(m ³ /day)	(mgd)
014	Strait of Juan de Fuca	32,000	8.4
015 ^{a/}	Port Angeles Harbor	2,300	0.6
016 ^{a/}	Port Angeles Harbor	1,900	0.5
017	Port Angeles Harbor	5,700	1.5
018	Port Angeles Harbor	57	0.015
019	Strait of Juan de Fuca	6	0.0015
020	Strait of Juan de Fuca	2,300	0.6
021	Port Angeles Harbor	950	0.25

^{a/} Combined flow rate

These discharges have a combined flow rate of 44,900 m³/day (11.87 mgd); 34,100 m³/day (9 mgd) is discharged to the Strait of Juan de Fuca, and the remaining 10,900 m³/day (2.87 mgd) is discharged into Port Angeles Harbor.

Outfalls 014, 019 and 020 created a large bright yellow plume of discoloration along the southern shore of the Strait of Juan de Fuca

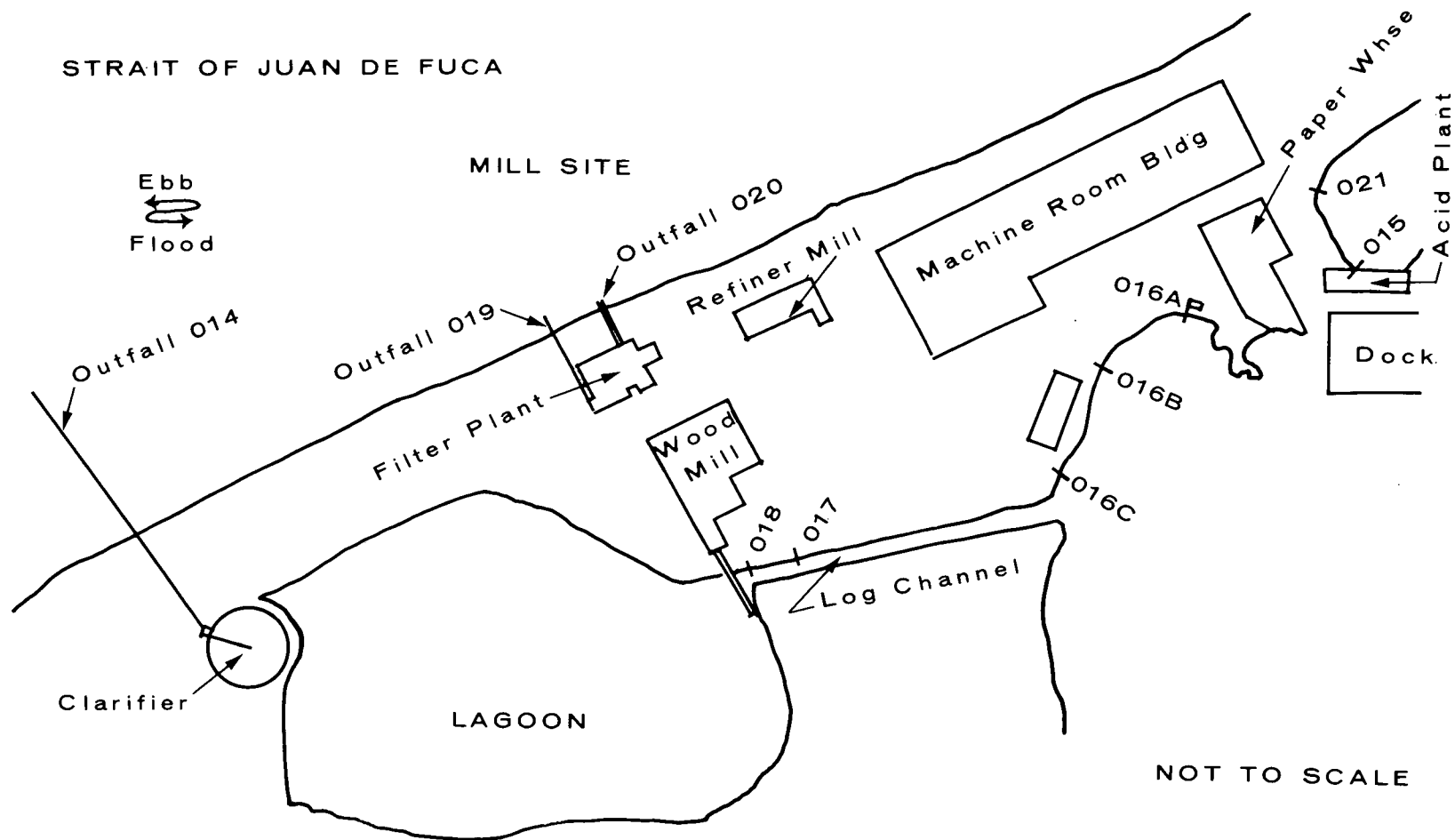
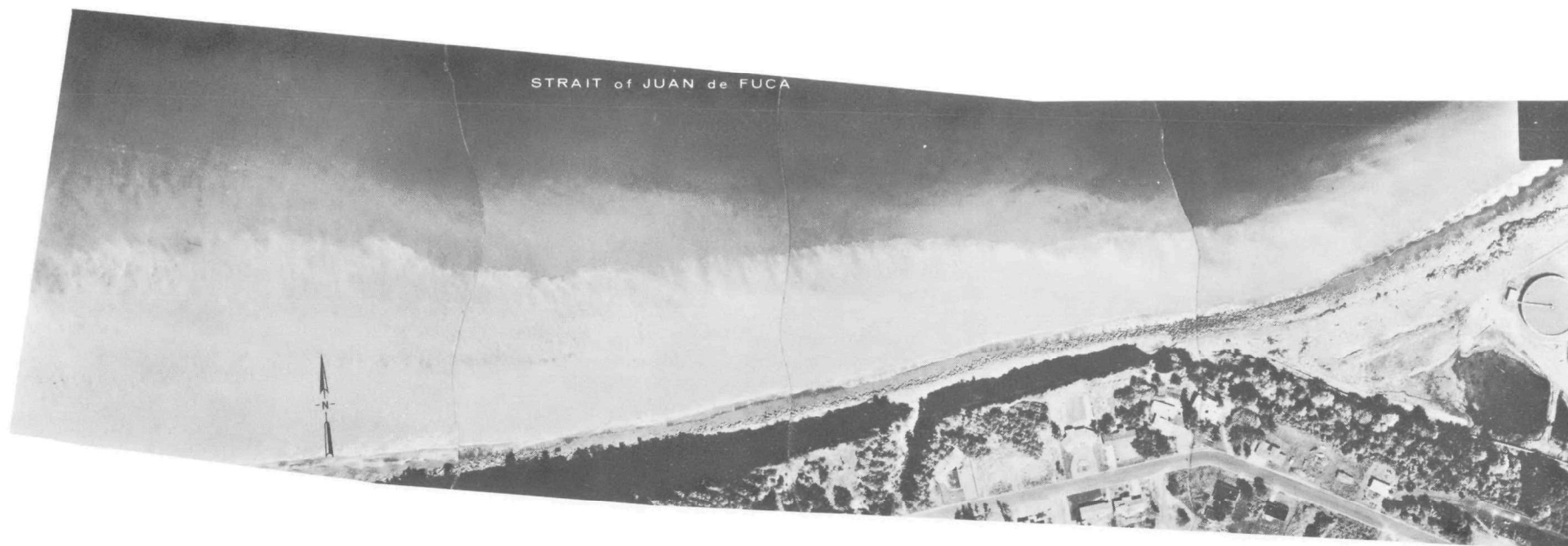


Figure IV-14. Crown Zellerbach Corporation Discharges



**Figure IV-15. Plume of Discoloration in Strait of Juan de Fuca
from Crown Zellerbach Corporation
(Facility Clarifier at far Right)**

[Fig. IV-15]. The waters along shore at the vertex of Port Angeles Harbor where outfalls 015, 016, 017, 018 and 021 were discharging were darker than the background waters further into the Harbor.

The total wastewater discharged from this facility consists of:

13% cooling water

1% boiler feed water

53% process water

33% other wastewater not specifically identified.

V. MODELING PORT ANGELES HARBOR

To understand the rationale in developing a model of the Harbor it is desirable to understand current motion in the ocean and the related equations of state. These equations will not be derived here and only those specialized cases which reflect the behavior of Port Angeles will be considered. Reference is made to hydrodynamics textbooks which furnish exact derivations, as well as textbooks of meteorology, which often prefer intuitive presentations.

MODELING ASSUMPTIONS

To develop a model for the effect of wind on water masses, three assumptions are made: 1) the internal pressure forces are neglected -- that is, there is no pileup of water against a land mass; 2) a homogeneous harbor is defined as one upon which a constant wind stress is acting as an external force; and 3) the turbulence of currents is described by the superposition of short, but intense, fluctuations of current velocity upon a relatively uniform motion which can be considered the actual oceanic current.

A pure drift current is the result of wind stress acting on the surface of the sea. This stress is produced either by friction of the air passing over the water, or by the pressure effect of the wind on waves which transfers part of the momentum of the wind to the water. Both effects usually act in the same direction and can be combined as a single resultant tangential force (force component parallel to the water's surface).

At the sea surface (northern hemisphere), the water in a pure drift current moves with a velocity V_0 in the direction of 45° cum sole* from the wind direction. At increasing depth the angle of deflection increases, and the velocity of the current rapidly decreases. At some depth D the deflection will amount to a full 180° and the velocity will have fallen to $e^{-\pi} = 1/23 V_0$. This velocity is small enough that by comparison with the surface value it can usually be neglected. The depth D can therefore be taken as a measure of the depth of penetration of the wind-generated ocean current. In general, it is also a measure of the depth to which the effect of a steadily flowing, horizontal layer penetrates into the adjacent water masses and was termed by Ekman^{3/} the "frictional depth." The equations for these parameters take the form:

$$V_0 = \frac{\pi \tau}{(2D\rho\omega \sin\phi)^{\frac{1}{2}}} \quad (4)$$

$$D = \left(\frac{\eta}{\rho\omega \sin\phi} \right)^{\frac{1}{2}} \quad (5)$$

Where: τ = shear stress
 ρ = density
 ω = angular velocity of the earth ($2\pi/86,400$ sec)
 ϕ = latitude (Coriolis effect)
 η = exchange coefficient for momentum (eddy coefficient or turbulent friction coefficient).

According to Equation 5, D is also a measure of the internal turbulent friction. It should be noted that the shear stress τ is not included in the equation relating D and η . This gives the indication that the vertical thickness of the current is independent of the wind intensity producing it and maintaining it against friction. Since the frictional

* In the direction of the apparent azimuth motion of the sun in equatorial plane.

coefficient n increases with wind strength, the frictional depth D will increase also. Figure V-1 shows the vertical structure of a pure drift current. The arrows projecting from the central column represent the direction and strength of the current at the surface at equidistant levels of $0.1D$, $0.2D$, etc. The arrowheads lie on a doubly curved spiral which when projected on the horizontal plane forms a logarithmic curve known as the Ekman spiral.

Equation 4 shows that the surface velocity is directly proportional to the shearing stress τ , but it is inversely proportional to the frictional depth D . The total water transport due to a drift current occurs perpendicular cum sole to the direction of the shearing stress of the wind producing it.

As long as the depth of water is greater than the frictional depth D , the vertical distribution of the drift current will be unaffected by the underlying surface, since the water layers below the frictional depths have an insignificant share in the drift current. When the depth of the water is about the same order as D , there is a noticeable effect on the drift current, and the trigonometric functions in Equations 4 and 5 are replaced by hyperbolic functions. The sea bottom represents a boundary to which the water adheres. When the water depth d is smaller than D the effect of the bottom will increase as the depth decreases.

Figure V-2 shows the vertical current structure for depths d equal to $1.25D$, $0.50D$, $0.25D$, and $0.1D$. The dashed curve near the origin shows the deviation from the curve $d = 1.25D$ for $d = 2.5D$. In practice there is no significant difference for even much greater values. The angle of deflection decreases rapidly with the depth of the water.

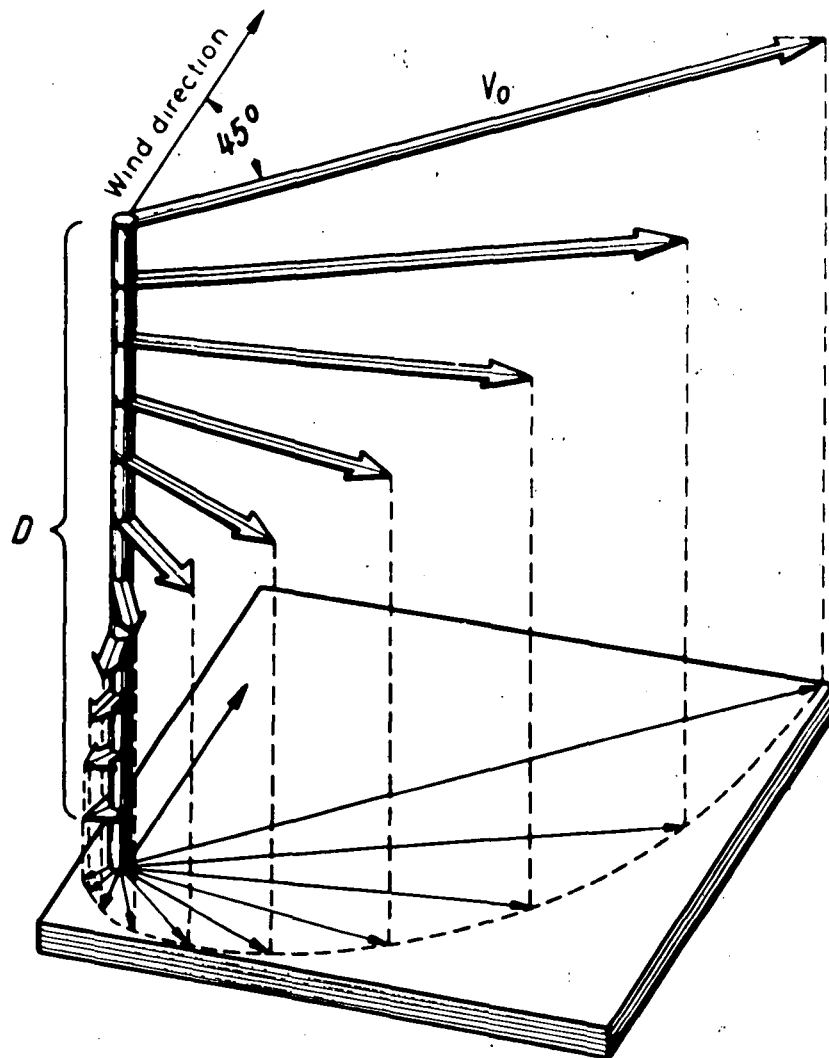


Figure V-1. Vertical Structure of a Pure Current
(According to Ekman) 4/

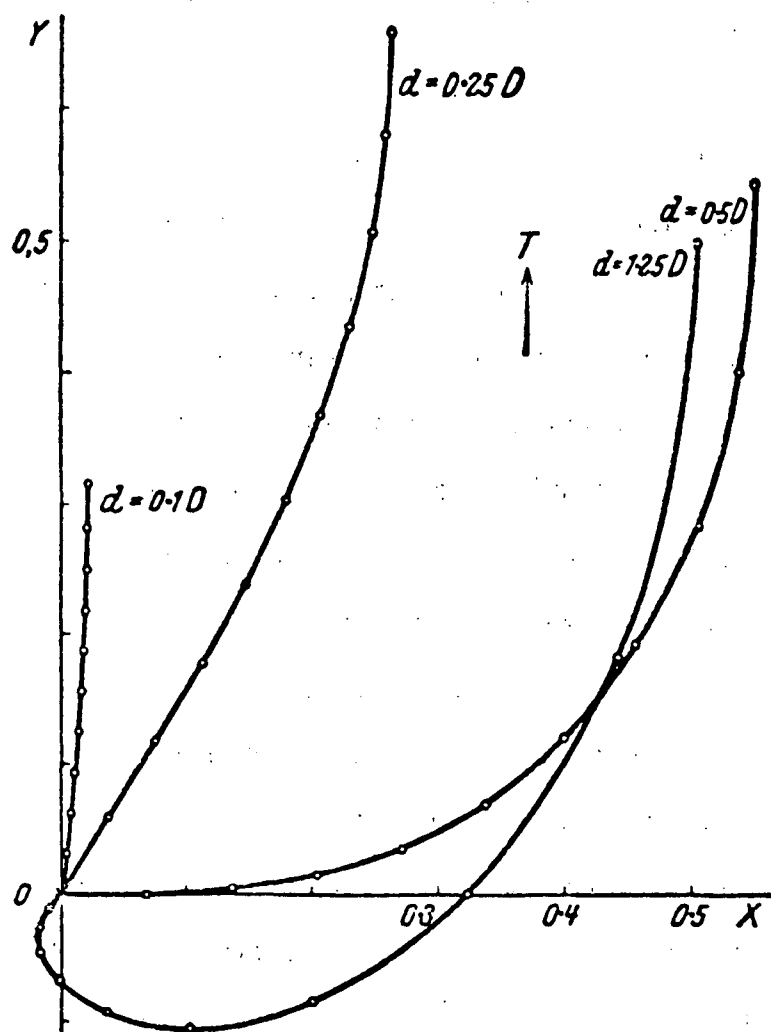


Figure V-2. Vertical Structure in Drift Currents for an Ocean Depth d Nearly Equal or Smaller than the Upper Frictional Depth D (10 Small Circles on Each Curve Indicate the End Points of the Velocity Vectors for the Depth $0.0, 0.1, 0.2 d$, etc.) ^{3/}

In very small depths ($d < 0.1D$), the deflection shows almost no effect of the earth's rotation.

THEORY VS. OBSERVATION

Comparison of the theory of drift currents with observations in the ocean is generally difficult because of simplifying assumptions. Shorelines of land masses or transport of the drift currents cause pileups of water which, in turn, induce currents that are included in the observations. Furthermore, the wind is not uniform over the ocean. If most of these difficulties are avoided by careful selection of the areas of observation, the results of the Ekman theory of drift currents can be confirmed. This is especially true for the angle of deflection α between the wind, W , and V_0 ; the ratio of current velocity to the wind velocity, V_0/W ; and the depth of frictional resistance D .

Port Angeles Harbor represents such a special case. Ediz Hook separates the Harbor from the effects of large-scale perturbations passing through the Strait of Juan de Fuca. Neither shoreline has any sharp protuberances; the Harbor is completely open to the east and the slope of the bottom is gentle with no projections. In addition, the meteorological data show that for this particular location the wind blows with great uniformity from the west. Compilation of data for such special cases^{4/} has shown the following relationship to be true:

$$V_0 = \lambda W / (\sin \phi)^{1/2} \quad (6)$$

where ϕ is the latitude, and λ a constant equal to 0.0126 when W is measured in cm/sec. As a rule of thumb, the drift velocity is approximately

does not agree with previous method

1.5 percent of the wind velocity in moderate and higher latitudes. It can also be shown that:

$$D = 7.6 W / \phi (\sin \phi)^{\frac{1}{2}} \quad (7)$$

from which follows

$$D = C' V_0 \quad (8)$$

where C' is a constant equal to

$$C' = 600 \frac{\text{m sec}}{\text{cm}} \quad (9)$$

Using mean monthly wind speed data [Table V-1] and taking $\sin \phi$ for the entrance to Port Angeles Harbor as 0.745 ($48^\circ 7' \text{ N}$), the values of D and V_0 for each month of the year are given in Table V-1. The agreement between the two methods of calculating V_0 is excellent. The last column of the Table was computed using a Harbor depth of 16 m.

Table V-1
Calculated Values of Frictional Depth and Current Velocity
Port Angeles Harbor

Month	W		$V_0 (\text{m/sec})$		D ($600 V_0$)	d
	(m/sec)	(kn)	.015 W	$\lambda W / (\sin \phi)^{\frac{1}{2}}$	(m)	
January	5.0	9.8	0.077	0.074	44	0.36D
February	4.2	8.2	.063	.061	37	.43D
March	4.5	8.7	.067	.066	39	.41D
April	5.0	9.8	.077	.074	44	.36D
May	6.1	11.9	.092	.089	54	.30D
June	6.1	11.9	.092	.089	54	.30D
July	7.1	13.8	.106	.104	62	.26D
August	5.4	10.5	.081	.079	47	.34D
September	4.1	8.0	.062	.060	36	.44D
October	3.5	6.8	.052	.051	31	.52D
November	3.8	7.4	.057	.056	33	.48D
December	4.5	8.7	.067	.066	39	.41D

Thus, using Figure V-2, during October when d was $0.52D$ the angle of deflection at the surface α is approximately 45° , at mid-depth it has increased to about 60° and at the depth of the outfall to 90° . This means that the direction of the current over the outfall would be directly south, while at the surface the transport would be southeast. In July when d is $0.26D$, the angle of deflection is only about 20° cum sole at the surface and 30° cum sole at the outfall.

These examples show the necessity for taking wind and current measurements concurrently. The last column of Table V-1 shows that during the course of a year d may be expected to vary between $0.26D$ and $0.52D$. Using July, the worst possible case, the frictional depth is still sufficiently shallow at this high latitude to allow the Coriolis effect to have a significant impact on the current in the Harbor.

In contrast to pure drift currents, pure gradient currents develop as a result of the wind piling up water at a shoreline, leading to an inclination of the sea surface. Where the actual depth is considerably less than the frictional depth in a homogeneous sea, as assumed for Port Angeles, the entire water column would behave as though it were gliding over the sea floor, retarded only by a slower moving boundary layer. In this case the Ekman effect would be negligible. Thus, if water motion in the Port Angeles Harbor were due to a gradient current induced by the piling up of water by either winds or tides, one would expect to find essentially uniform motion throughout the entire water column.

EVALUATION OF THE MODEL

Because data collection was not specifically designed to determine the type of current existing in the Harbor, it is difficult to state conclusively that a pure drift current resulting in the Ekman spiral exists in Port Angeles Harbor. To a certain extent, it is easier to indicate the current patterns that do not exist. Although the water in the basin was shown to be homogeneous by data presented earlier, close examination of the current roses in the ITT Rayonier report failed to reveal a single case of uniform unidirectional flow throughout the water column. On only a few occasions was a substantial portion of the water column moving uniformly in direction and speed.

Topographically the Harbor is a broad, shallow basin with gentle geographic features open to the Strait of Juan de Fuca and the passing tides. Yet, the water does not simply oscillate in and out of the basin. If the Harbor were rugged, with many barriers to the flow building up actual heads of water and resulting in the tidal bores that occur in many estuaries, an argument could possibly be made for the complicated circulating patterns in the Harbor.

Since these two possible models of circulation for the Port Angeles basin do not occur, it seems reasonable to accept that the wind produces a drift current with a resulting Ekman spiral, as suggested although not proven by the data.

Tidal velocities and headings at 10 m (33 ft) in the ITT Rayonier report for Station 4 [Fig. III-1] show that the majority of time current flow was slightly south of due west. This indicates that at this depth the outfall was located sufficiently north of the Ekman spiral to allow water moving into the Harbor to replace the water flowing out along the south shore in the drift current. Thus, the pollutants would be carried into the Harbor, then southward to the shore, then eastward along the shore past Morse Creek toward Green Point. In fact, the data indicate that for only a few minutes during the afternoon of 5 November 1970 did the waterflow across the outfall correspond to that which the ITT report claimed was the predominant flow -- a northward flowing anticyclonic motion across the outfall.

Station 3 is of interest because it should be located within the drift current, if one exists. The continuous current readings for Station 3 were also taken only at 10 m. Accepting the mean wind values given for September and October, and the values of D calculated from Table V-2, it is possible to calculate the drift current heading and relative velocity for this station at 10 m. Since the station was close to the bottom of the Harbor (12 m; 40 ft), d is about $0.33D$ to $0.39D$ (September-October). From Figure V-2, one would expect α at 10 m to be about 20° cum sole to the wind which is coming from the west at 90° relative to the compass. Tidal heading for the station shows that except for the period of about an hour and a half on the afternoon of 30 September 1970 the current was within $\pm 10^\circ$ of the predicted 110° given by the model at all times.

Table V-2

U.S. DEPARTMENT OF COMMERCE, WEATHER BUREAU IN COOPERATION WITH
THE WASHINGTON STATE DEPARTMENT OF COMMERCE AND ECONOMIC DEVELOPMENT
CLIMATOGRAPHY OF THE UNITED STATES 20-45

LATITUDE 48° 07'
LONGITUDE 123° 26'
ELEV. (GROUND) 99 ft.

CLIMATOLOGICAL SUMMARY
NORMALS, MEANS, AND EXTREMES

STATION PORT ANGELES, WASH.

Month	Temperature								Normal degree days	Precipitation										Relative humidity				Wind					Average sky cover sunrise to sunset	Mean number of days													
	Normal				Extremes					Normal total	Maximum monthly	Year	Minimum monthly	Year	Maximum in 24 hrs.	Year	Snow, Sleet					4:30 A. PST	10:30 A. PST	4:30 P. PST	10:30 P. PST	Mean hourly speed	Prevailing direction	Fastest mile			Clear	Sunrise to sunset			Precipitation .10 inch or more	Snow, Sleet 1.0 or more	Thunderstorms	Heavy fog	Max. temp. 90°	32°	Min. temp. 32°	Zero	
	Daily maximum	Daily minimum	Monthly	Record highest	Year	Record lowest	Year	Mean total									Maximum monthly	Year	Maximum in 24 hrs.	Year	Speed							Direction		Year		Partly cloudy	Cloudy										
(a)	30	30	30	30	1950	30	30	30	30	1954	30	1942	30	1935	30	30	30	1950	6.5	1952	82	78	77	82	9.7	SSE	52	WSW	1951	8.2	3	4	24	9	3	0	1	0	2	11	0		
J	43.7	33.5	38.6	62	1960	7	1950	818	3.87	11.06	1954	.90	1942	3.02	1935	4.4	38.8	1950	6.5	1952	82	78	77	82	9.7	SSE	52	WSW	1951	8.2	3	4	24	9	3	0	1	0	2	11	0		
F	46.0	34.5	40.3	67	1941	12	1933	692	3.06	6.97	1949	.84	1956	3.30	1949	1.8	15.1	1949	7.0	1940	84	77	77	84	8.2	N	49	NSW	1952	8.0	3	4	21	7	*	0	1	0	*	9	0		
M	48.8	36.3	42.6	66	1930	21	1951	694	1.99	4.26	1950	.57	1944	1.55	1948	.6	9.2	1951	7.0	1955	84	76	75	83	8.7	N	53	N	1951	8.0	3	6	22	5	1	0	1	0	0	7	0		
A	54.2	40.1	47.2	74	1955	25	1936	534	1.08	2.50	1937	.09	1956	.91	1948						82	72	71	82	9.8	N	44	WNW	1952	7.1	5	7	18	4	0	0	1	0	0	1	0		
M	59.5	44.5	52.0	83	1956	30	1954	403	.89	2.49	1948	.07	1935	1.00	1948						85	75	74	84	11.8	N	41	WNW	1951	6.8	5	11	15	3	0	1	2	0	0	*	0		
J	62.8	48.6	55.7	89	1958	37	1933	279	.96	3.35	1931	.01	1934	1.33	1946						88	77	75	84	11.2	N	38	N	1952	6.3	7	9	14	3	0	1	3	0	0	0	0		
J	66.5	51.1	58.8	93	1941	41	1954	195	.48	1.30	1955	.00	1958	.48	1954						89	79	76	86	13.8	N	38	N	1951	5.4	10	10	11	2	0	1	5	*	0	0	0		
A	66.4	51.0	58.7	87	1952	41	1953	195	.58	2.23	1954	.02	1955	.65	1956						92	81	79	89	10.5	N	43	N	1951	5.9	9	8	14	2	0	1	10	0	0	0	0		
S	63.6	48.5	56.1	85	1955	37	1937	267	1.10	3.09	1933	.04	1939	1.23	1953						89	78	78	88	8.0	N	41	WNW	1951	5.5	9	9	12	3	0	*	8	0	0	0	0		
O	56.6	43.6	50.1	81	1936	24	1935	462	2.48	7.75	1956	.25	1936	2.05	1947						88	80	81	88	6.8	N	47	N	1951	7.4	5	7	19	7	0	0	5	0	*	*	0		
N	49.1	38.2	43.7	67	1950	12	1955	639	3.77	8.44	1958	.60	1943	2.42	1955	.6	7.5	1946	4.5	1946	86	80	81	85	7.4	N	40	NSW	1952	8.3	2	5	23	9	0	0	2	0	*	4	0		
D	46.0	36.0	41.0	67	1940	17	1956	744	4.35	10.83	1933	1.11	1935	2.63	1937	1.1	7.9	1949	4.5	1949	86	81	81	84	8.7	NSW	58	E	1951	8.6	1	4	26	10	1	0	1	0	*	8	0		
Yr.	55.3	42.2	48.7	93	1941	7	1950	5922	24.61	11.06	1954	.00	1958	3.30	1949	8.5	38.8	1950	7.0	1955	86	78	77	85	9.6	N	58	E	1951	7.1	62	84	219	64	5	4	40	*	2	40	0		

(a) Length of record, years. (1931-1960)

+ Also on earlier dates, months, or years.

T Trace, an amount too small to measure.

* Less than one half.

Data recorded at Weather Bureau Office located at the USCG Air Station during period 1947-1952.
Data entered in column "Fastest Mile" are for the fastest observed mile during 2-year period 1951-1952. Station was not equipped with automatic recording wind equipment.

Similar calculations for October indicate that α is only a few degrees larger and that essentially the same correlation holds for 1 October 1970. On 2 October the basic direction of flow at 10 m (33 ft) was between west and west-southwest. The model may have failed because of calm wind conditions or because a strong tidal component was imposed upon the Ekman spiral. This does not invalidate the long-term net transport of the spiral. V_0 is predicted to be 0.060 m/sec (0.12 kn) for September and .051 m/sec (0.10 kn) for October [Table V-1]. If this were a drift current one would expect current values at 10 m to remain considerably below these values, and in fact that was the case. If it were a pure gradient current, one would expect essentially the same flow rate at 10 m as at the surface, which was not the case.

The dye tracers released on the surface provided the only estimate of V_0 in the ITT Rayonier study. These reflected the predicted motion in three out of four cases. Figure III-5 shows that dye was released at a point between Stations 2 and 3. On 29 and 30 September, and 2 October 1970 the dye moved east by southeast along the shore toward Morse Creek with surface velocities of 0.061, 0.025 and 0.088 m/sec (0.118, 0.049, 0.171 kn), respectively. These correspond reasonably well to the predicted value range of 0.051 to 0.061 m/sec (0.099 to 0.118 kn), particularly against a flood tide. On 2 October, when the dye moved directly across the mouth of the Harbor near Ediz Hook [Fig. III-6], the model may have failed because of a shift in or lack of wind or tidal conditions -- in contrast to the other three studies which took place during flood tide.

Each time a long-term change in the direction of wind velocity occurs, the current vectors must be reestablished. Figure V-3 shows the adjustment the current vector V_0 follows after the onset of wind. As the wind velocity changes in speed but not in direction, the depth of the frictional resistance D likewise varies. Thus, current vectors at depth will change from either a shift in wind speed or direction.

Since the ITT Rayonier drogue studies were all conducted at the 4 m (13 ft) depth, the data are not sufficient to show rotary motion throughout the column, as in the Ekman spiral. Here again, if gradient currents alone were acting one would expect all of the drogues to move uniformly in the same direction. However, the only cases in which this occurred were where the drogues were released within the Strait of Juan de Fuca. Even in these cases when the drogues entered the Harbor random motion developed, indicating the lack of gradient currents within the basin. On several days, such as 20 and 28 August, drogue motion clearly followed that which was predicted. Again, lack of wind data and surface drogues makes it impossible to validate or reject the model.

The dispersion of the test dye injected into the city of Port Angeles sewage outfall [Table III-2] was so rapid that rotary motion with its attendant turbulence was indicated, rather than the laminar flow associated with gradient currents.

Wind speed and direction on the days of the remote sensing survey were calm. This is unfortunate since the model assumes a constant wind stress. However, Figure IV-4 reflected primarily tidal motion, except

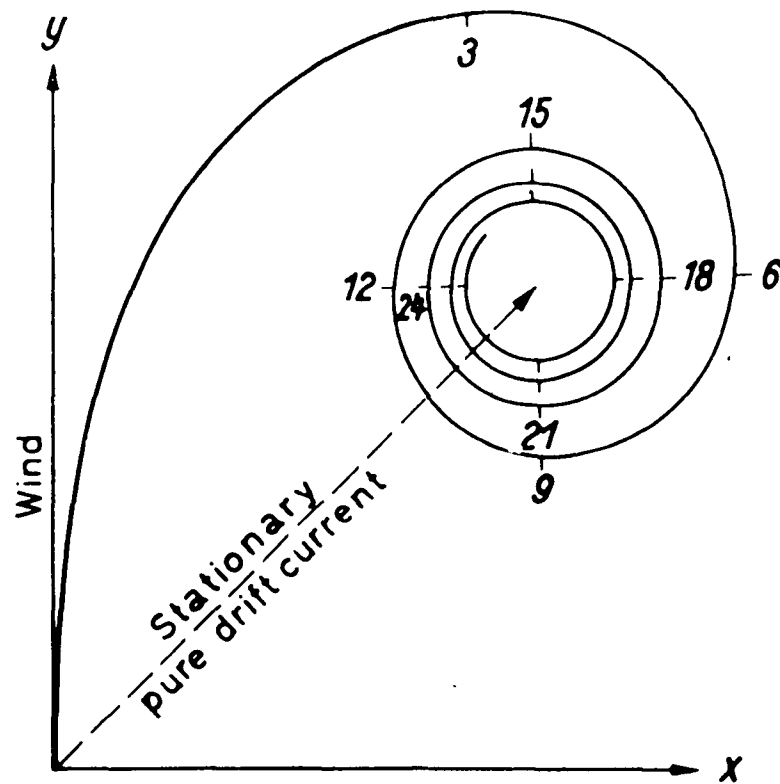


Figure V-3. Adjustment of the Current Vector, at the Sea Surface, to a Stationary Position After Onset of the Wind (Ekman, 1927) 4/

for cyclonic motion of the 12 m (40 ft) drogue. The latter case was probably a result of residual motion of the Ekman spiral that had not completely decayed since the wind ceased.

A visual inspection was made of Port Angeles Harbor on 28 December 1973, and numerous photographs were taken of the water surface to record the movement of surface slicks. The wind was directly from the west at about 5 m/sec (10 kn). Surface slicks or films formed straight lines several miles long, drifting east by southeast in the southern half of the Harbor. These streaks, each a few yards wide, joined near Green Point, then traveled as one large slick northeast into the Strait of Juan de Fuca. The motion of the slicks reflects the motion of the surface layer immediately beneath them. On the north side of the Harbor, slicks were broad and diffused as they appeared to be forced into the wind. This reflects an eddy pattern where water enters the Harbor on the north side around Ediz Hook, moves counterclockwise across the Harbor, and then moves out of the Harbor along the southern shore, completing the gyre.

REFERENCES

1. *Pollution Effects of Pulp and Paper Mill Wastes in Puget Sound*, U. S. Dept. of the Interior (Federal Water Pollution Control Administration Northwest Regional Office, Portland, Oreg.; Washington State Pollution Control Commission, Olympia), March 1967, 474p.
2. *Outfall Location Studies, Port Angeles, Washington*, ITT Rayonier Inc., Olympic Research Division, Shelton, Wash., August 1971, 450p.
3. Defant, Albert, *Physical Oceanography*, Vol. 1, Pergammon Press, New York, 1961, p. 401.
4. Dietrich, Günter, *General Oceanography*, John Wiley & Sons, New York, 1963, 588p.

APPENDIX A
REMOTE SENSING TECHNIQUES

Aircraft and Sensor Data
Data Interpretation and Analysis
Error Analysis
Film Spectral Sensitivity Data
Optical Filter Transmittance Data
Development Process for Reconnaissance Films
Focal Length, Angle of View

REMOTE SENSING TECHNIQUES*

AIRCRAFT AND SENSOR DATAAircraft and Flight Data

A high-performance aircraft, specifically designed and equipped for aerial reconnaissance work, was used for the remote sensing flights.

The aircraft was used for day and night flights over Port Angeles Harbor.

The flight parameter data that specify the values of the aerial reconnaissance variables are summarized in Table A-1. These variables are important at the time the mission is flown and during the analysis of the airborne data. With rare exception, the airspeed variations are automatically processed in the aircraft computer system and, combined with aircraft altitude, are used to calculate the amount of photographic stereo overlap.

Cameras

Three cameras and an infrared line scanner (IRLS) were the sensors on board the aircraft. The cameras were KS-87B aerial framing cameras equipped with 152 mm (6 in.) focal length lens assemblies. They were mounted in the aircraft in their respective vertical positions as shown in Figure A-1.

The viewing angle of the KS-87B framing cameras was 41° centered about the aircraft's nadir as shown in Figure A-2. A diagram of a typical framing camera is shown in Figure A-3.

*Mention of equipment and/or brand names in this report does not constitute endorsement or recommendation by the Environmental Protection Agency.

Table A-1
Flight Parameter Data
Port Angeles Harbor

Parameter	Date	
	25 April 1973	25 July 1973
Time of Flight	(Day) 1120 to 1250 PST (Night) 2012 to 2128 PST (Night) 2337 to 2451 PST	(Day) 1200 to 1330 PDT (Day) 1520 to 1637 PDT (Day) 1640 to 1730 PDT
Air Speed	325 kn	325 kn
Altitude Above Ground Level	(Day) 457 m (1,500 ft) (Night) 305 m (1,000 ft)	457 m (1,500 ft) --
Sensors	(Day) A11 (Night) IRLS	(Day) A11 --

LEGEND

- 1 KS-87 FRAMING CAMERAS
- 2 INFRARED LINE SCANNER

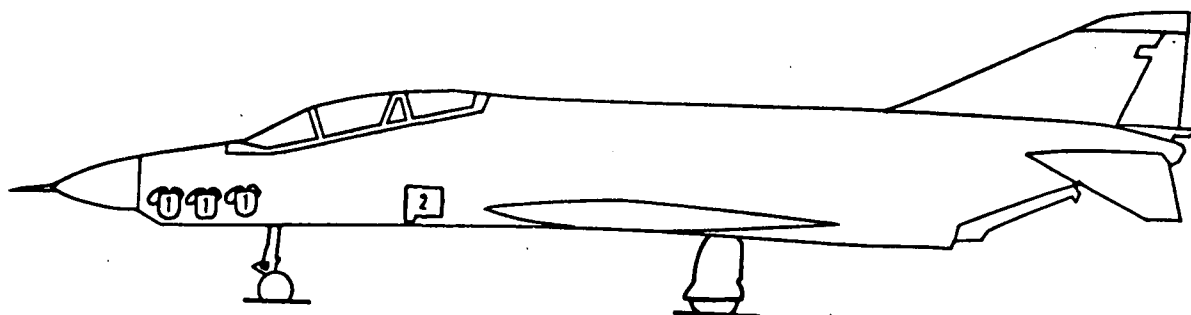


Figure A-1. Aircraft Sensor Locations

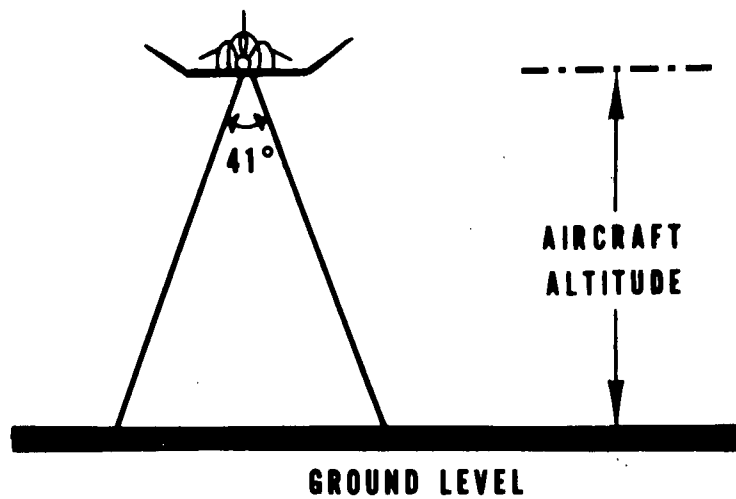
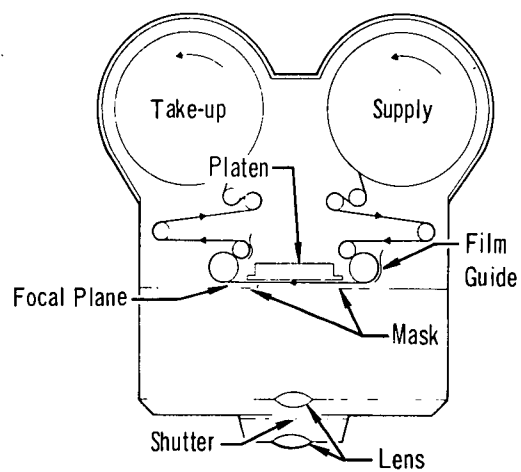


Figure A-2. Viewing Angle of Framing Camera



Film Advances Frame by Frame

Figure A-3. Framing Camera

Films and Filters

The cameras were loaded with the following film and optical filter combinations:

Camera Station 1 -- Kodak S0-597 Aerographic Ektachrome Film (127 mm; 5 in.) with a Wratten HF-3/HF-5 gelatin optical filter combination. The film provides a true color transparency 114 mm sq (4.5 in. sq). The filter combination prevents ultraviolet light from reaching the film and eliminates the effects of atmospheric haze.

Camera Station 2 -- Backup sensor for Camera Station 1.

Camera Station 3 -- Kodak 2443 Aerochrome Infrared Film (127 mm) with a Wratten 16 gelatin optical filter. The film provides color transparencies 114 mm sq.

The Wratten 16 filter (deep orange in color) transmits a portion of the visible optical spectrum (i.e., deep green, yellow, orange, and red) as well as the near-infrared energy from 7.0 to 1.0 μm . The film presents a modified-color or false-color rendition in the processed transparency unlike the more familiar true-color films. It has an emulsion layer that is sensitive to the near-infrared in addition to the red and green layers, whereas the true-color ektachrome films have red, green, and blue sensitive layers. (Every color film has various combinations of red, green, and blue dyes similar to the red, green and blue dots on the front of a color television picture tube.) The modified or false-color rendition comes into play when the exposed image on the infrared

film is processed. In the finished transparency, the scene objects (trees, plants, algae) producing infrared exposure appear red, while red and green objects produce green and blue images, respectively. Most important, this film records the presence of various levels of chlorophyll in terrestrial and aquatic plant growth. The leaves on a healthy tree will record bright red rather than the usual green; unhealthy foliage will appear brownish-red. The orange filter keeps all blue light from reaching the film to prevent unbalance in red, green, and blue.

Infrared Line Scanner

The aircraft was equipped with an AN/AAS-18 Infrared Line Scanner (IRLS) which images an area along the flight path of the aircraft. The width of the image area depends upon aircraft altitude; the area is encompassed by a 120° field-of-view in crosstrack, or perpendicular to the flight path [Fig. A-4].

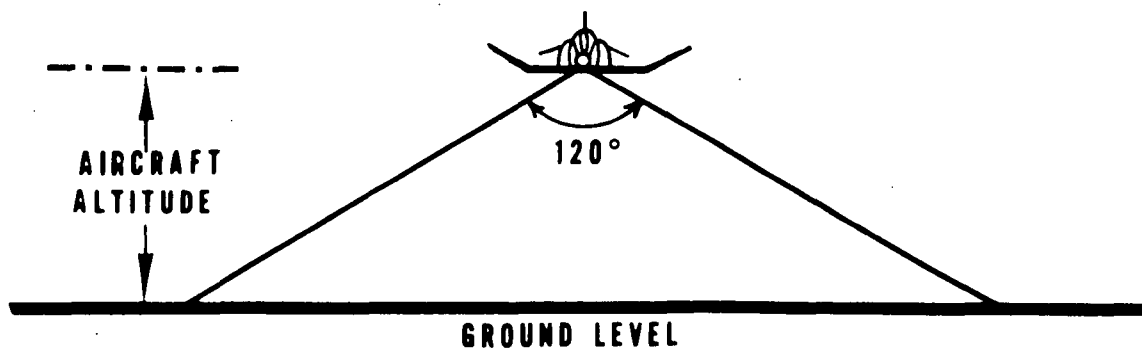


Figure A-4. Field of View of IRLS

An IRLS converts variations in infrared energy emissions from objects of different temperatures into a thermal map. The three basic parts of an IRLS are the scanner optics, a detector array, and a recording unit. The scanner optics collect the infrared emissions from ground and water areas and focus them on the detectors [Fig. A-5].

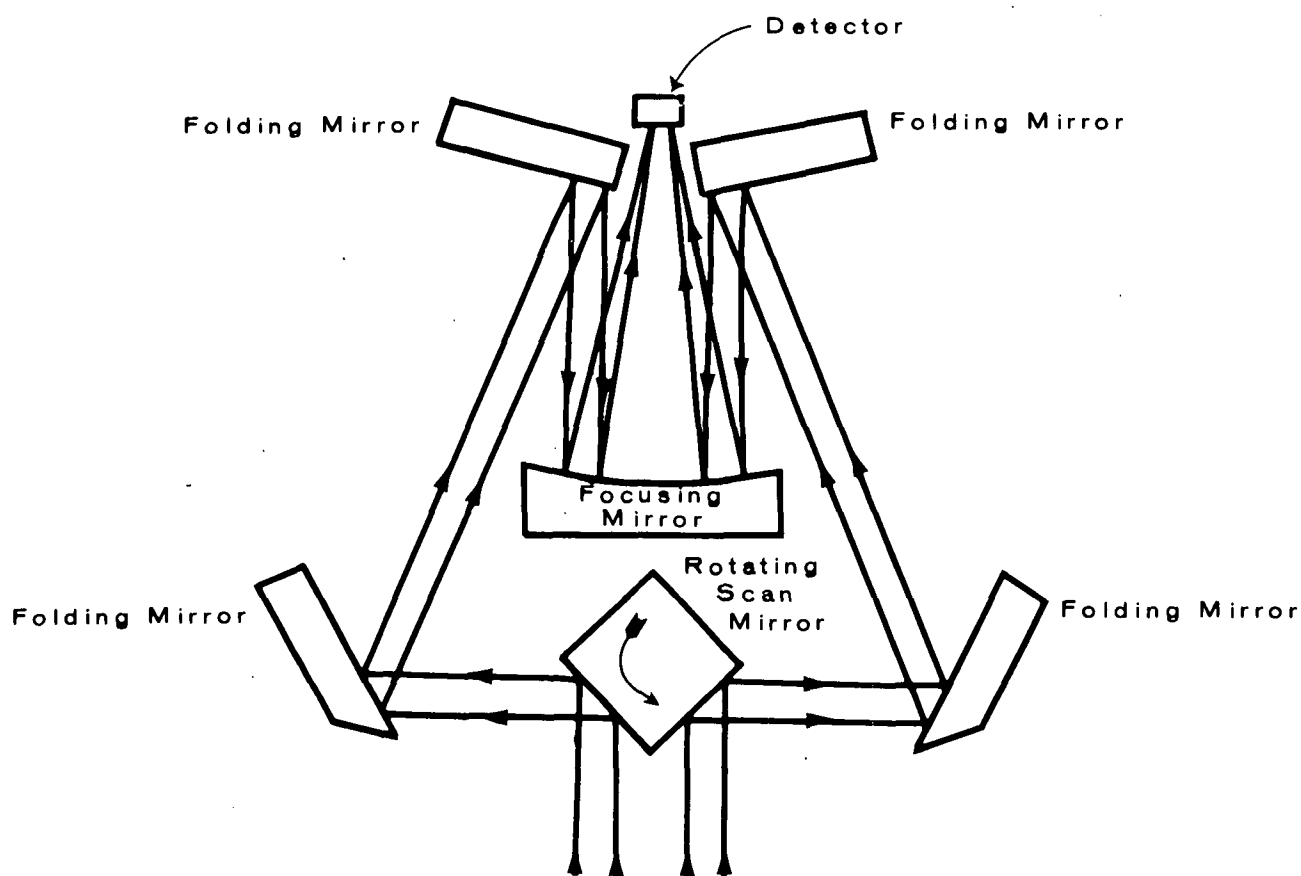


Figure A-5. IRLS Optical Collection System

The detectors, cryogenically cooled to 26° K, convert the infrared energy collected by the scanner optics into an electronic signal. This signal is processed electronically and subsequently transformed into visible light through a cathode ray tube. This light is recorded on ordinary 126 mm (5 in.) RAR black-and-white film. The recorded thermal map is 100 mm (4 in.) wide and its length depends upon the length of a particular line of flight being imaged.

The IRLS has a sensitivity bandwidth from 8 to 14 μm , the so-called thermal band of the electromagnetic spectrum. Applying Wien's Displacement Law, this represents a temperature band from -66° to 89° C. The system has an instantaneous field-of-view of 1 mrad sq. The total field-of-view is achieved by the rotating mirror in the optical collection system, which is 120° x 1 mrad. The measured noise equivalent temperature (N.E.T.) of the IRLS is 0.32° C with 100 percent probability of target detection. This represents an effective measurement of the temperature resolution of the system.

DATA INTERPRETATION AND ANALYSIS

Data is interpreted and analyzed on the original photographic and Infrared Line Scanner (IRLS) films; prints of duplicated transparencies degrade the image in scale and color balance. The original films are: true color transparencies, false color infrared transparencies, black-and-white ultraviolet negatives and the IRLS thermal image black-and-white negatives.

Standard image analysis techniques were employed in the reduction of distances/areas and stereoscopic analysis of areas displaying topographic gradients on land and in the water. The reduced data were subsequently plotted on U. S. Geological Survey 7.5 minute topographic maps (scale 1:24,000) and U. S. Coast Guard and Geodetic Survey Nautical Charts (scale 1:10,000). To evaluate scale consistency, the map scales were compared to the imagery empirical scales derived from the optical focal length of each sensor and the altitude of the aircraft above water level.

A Macbeth TD-203AM Densitometer was employed during the analysis of the color films to measure film densities as a function of the three cardinal colors -- red, blue and green. This system measures film densities with an accuracy of 0.02 density units and a measurement repeatability of 0.01 density units.

Temperature levels are represented on black-and-white IRLS film by various shades of gray in the negative. Areas of low density (clear film) represent cooler temperatures, and as the temperature of a particular target becomes warmer the density of gray in the film also increases. Positive prints presented in this report reflect the reverse of the negative film. Cool areas are dark while the warm areas are light gray.

It is important to note that the IRLS will only record water surface temperatures since water is opaque in this region of the infrared spectrum. The maximum depth penetration in either fresh or salt water is 0.01 cm. Therefore, a submerged thermal discharge can be detected from an aircraft with an IRLS only if the warm wastewater reaches the surface of the receiving waters.

DEVELOPMENT PROCESSES FOR BLACK-WHITE
AND COLOR RECONNAISSANCE FILMS

The film was processed in Eastman Kodak Company processors. The infrared and true-color Ektachrome films were processed in the Ektachrome RT Processor, Model 1811, Type M, Federal Stock Number 6740-109-2987PK, Part Number 460250. This machine uses Kodak EA-5 chemicals. The temperature of the respective chemicals in the processor and the film process rate, in ft/min, are the important parameters. Their values were specified as follows:

Prehardener	115°F
Neutralizer	115°F
First Developer	115°F
First Stop Bath	115°F
Color Developer	120°F
Second Stop Bath	120°F
Bleach	125°F
Fixer	120°F
Stabilizer	120°F

The film process rate was 9 ft/min. The nine chemical baths, mentioned above, comprise the EA-5 process used for the color films. The temperature and pressure of the fresh water supplied to the processor was 120°F and 45 psi minimum, respectively. The fresh water is used to wash the film immediately before entering the dryers.

FILM SPECTRAL SENSITIVITY DATA
OPTICAL FILTER TRANSMITTANCE DATA

The spectral curves for each film and optical filter used during this reconnaissance program are provided on the following pages:

S0-397 with HF3/HF5 filter combination

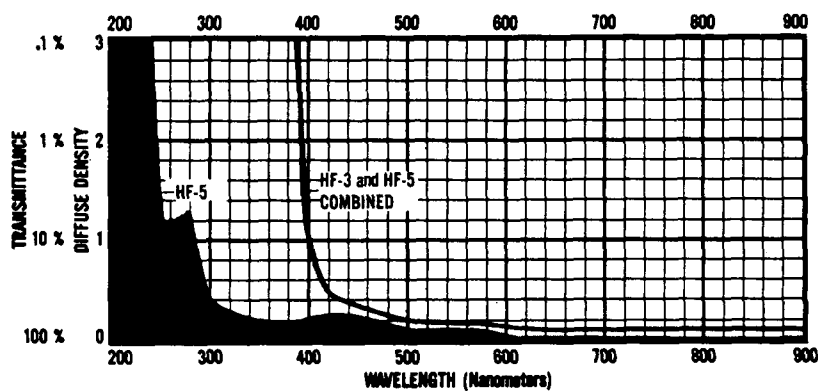
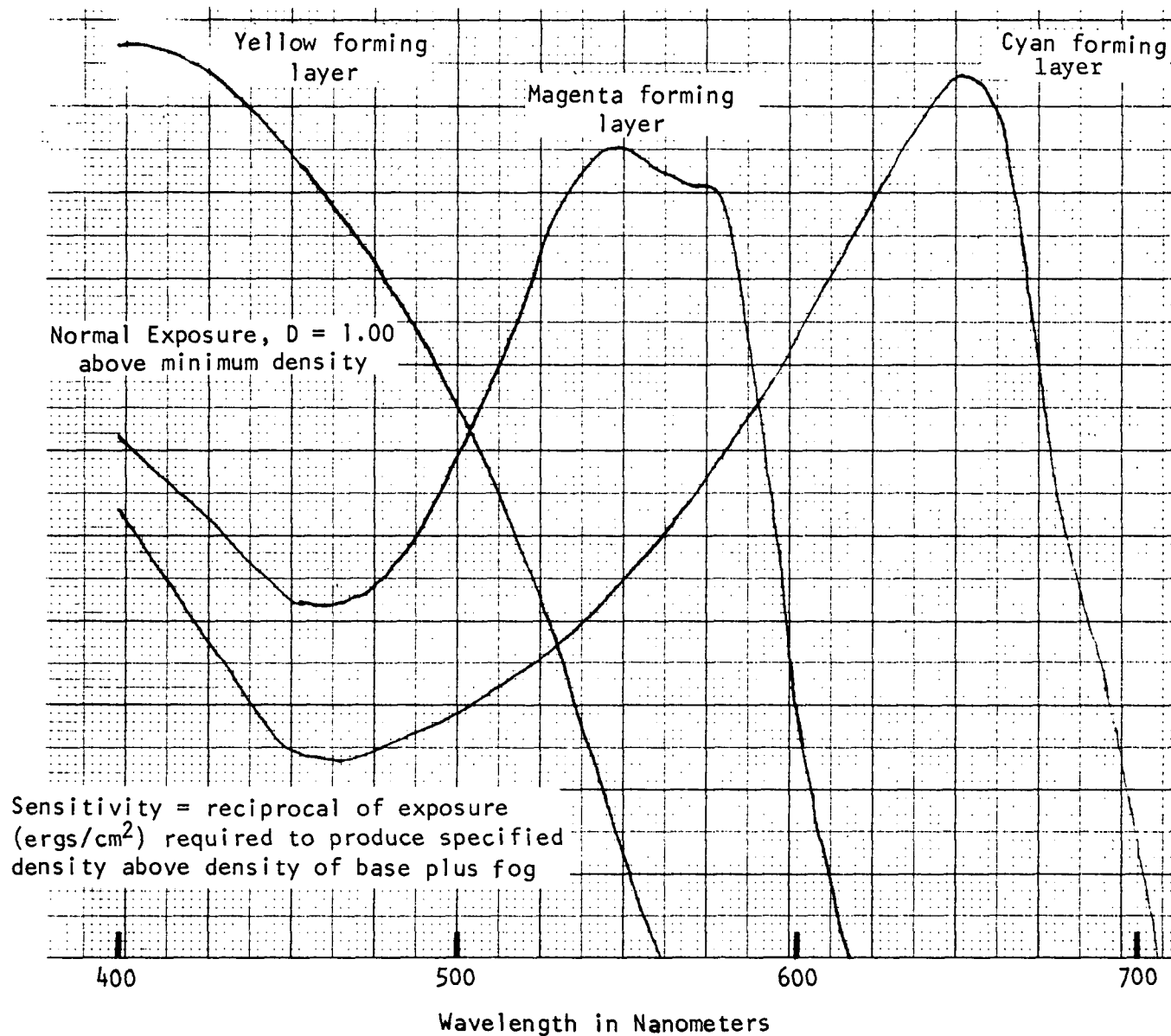
2443 with 16.

To obtain the optical band width $B(\lambda)$ of each film-filter combination let $F(\lambda)$ be the transmittance function of the respective filter and $S(\lambda)$ be the spectral sensitivity function for the particular film.

Then:

$$B(\lambda) = \int_{\lambda_1}^{\lambda_2} S(\lambda) F(\lambda) d\lambda.$$

Kodak Ektachrome EF Aerographic Film
S0-397 Development Process EA-5



**HF-3
and
HF-5**

AAB *

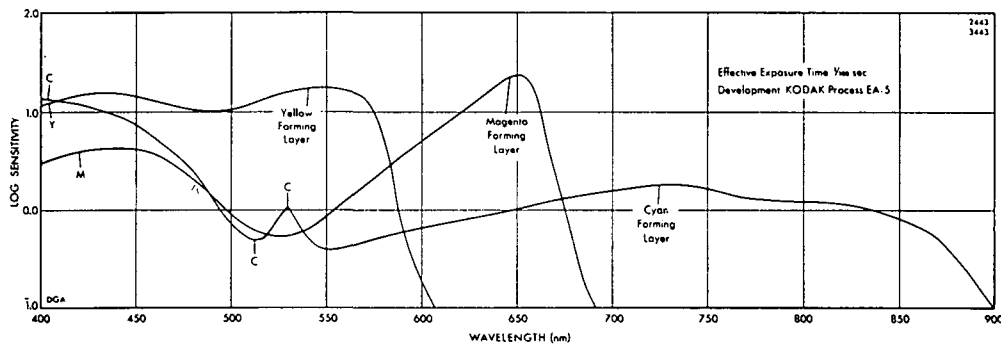
INFRARED-SENSITIVE FILMS

KODAK AEROCHROME Infrared Film 2443
(ESTAR Base)

KODAK AEROCHROME Infrared Film 3443
(ESTAR Thin Base)

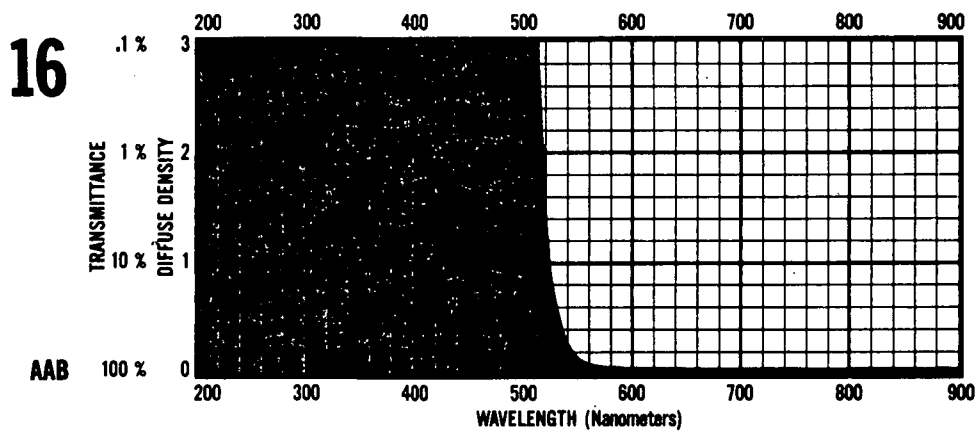
Critical users of these two films should determine the actual sensitometric characteristics of their particular batch of film by using their own specialized techniques. The keeping conditions for these films have an effect on their sensitometric response.

Spectral Sensitivity Curves:



Sensitivity = Reciprocal of the exposure (ergs/cm²) required to produce a density of 1.0 above D min. Measurements were confined to the 400 to 900 nanometer region.

Spectral Dye Density Curves:



Orange. Permits greater overcorrection of sky than No. 15. Absorbs small amount of green.

ERROR ANALYSIS

Limitations can be placed on the accuracy or uncertainty of the film analysis measurements carried out on the photographic and thermal data. Measurements for linear distance and surface area were made with scaling instruments and light table microscopes.

The uncertainty for linear distance (ΔLD) is:

$$\Delta LD = \pm 2 \times 10^{-4} \times \text{photographic scale (meters)} \quad (1)$$

The photographic scale for this study was 1:3,000. The value for $\Delta LD = (\pm 2 \times 10^{-4} \times 3,000) \text{ m} = \pm 0.6 \text{ m}$. A distance X , measured on the original photographic film, is accurate to within $\pm 0.6 \text{ m}$.

The uncertainty for the surface area (ΔSA) is (rectangular):

$$\Delta SA = \pm \Delta LD (\pm X \pm Y) \quad (2)$$

For this study $\Delta SA = \pm 0.6 (\pm X \pm Y) \text{ m}^2$, ($\Delta LD = \pm 0.6 \text{ m}$).

For example, a rectangular area with dimensions of $X \pm 0.6 \text{ m}$ and $Y \pm 0.6 \text{ m}$, would have the value $[XY + 0.6(\pm X \pm Y) \pm 0.36] \text{ m}^2$.

The uncertainty in the IRLS is the measured system noise equivalent temperature which is $\pm 0.32^\circ\text{C}$.

No atmospheric corrections were applied to the reconnaissance data under the assumption that the atmospheric effect was constant through the air column between the aircraft and the water during the short duration of each phase of the mission.

FOCAL LENGTH, ANGLE OF VIEW
AND THE EFFECTS OF FOCAL LENGTH AND ALTITUDE

The focal length of the aerial sensors affects the size (or scale) of the resulting imagery. At any given altitude, the image size changes in direct proportion to changes in focal length. Also, for a given focal length the image size is inversely proportional to the altitude.

The angle of view of a sensor is a function of the focal length and the image format size. The importance of the angle of view is its relationship to the amount of target area recorded in the imagery. Refer to the following diagrams: A. Focal length of a simple lens. B. Effect of focal length on scale and ground coverage. C. Effect of altitude on scale and ground coverage.

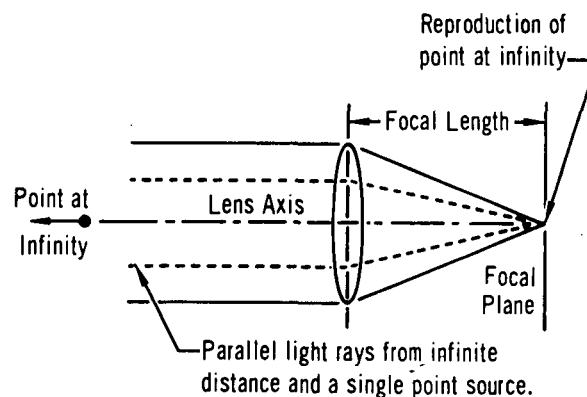


Diagram A. Focal Length of a Simple Lens

Focal length is the distance from the lens (A) to the film (B).

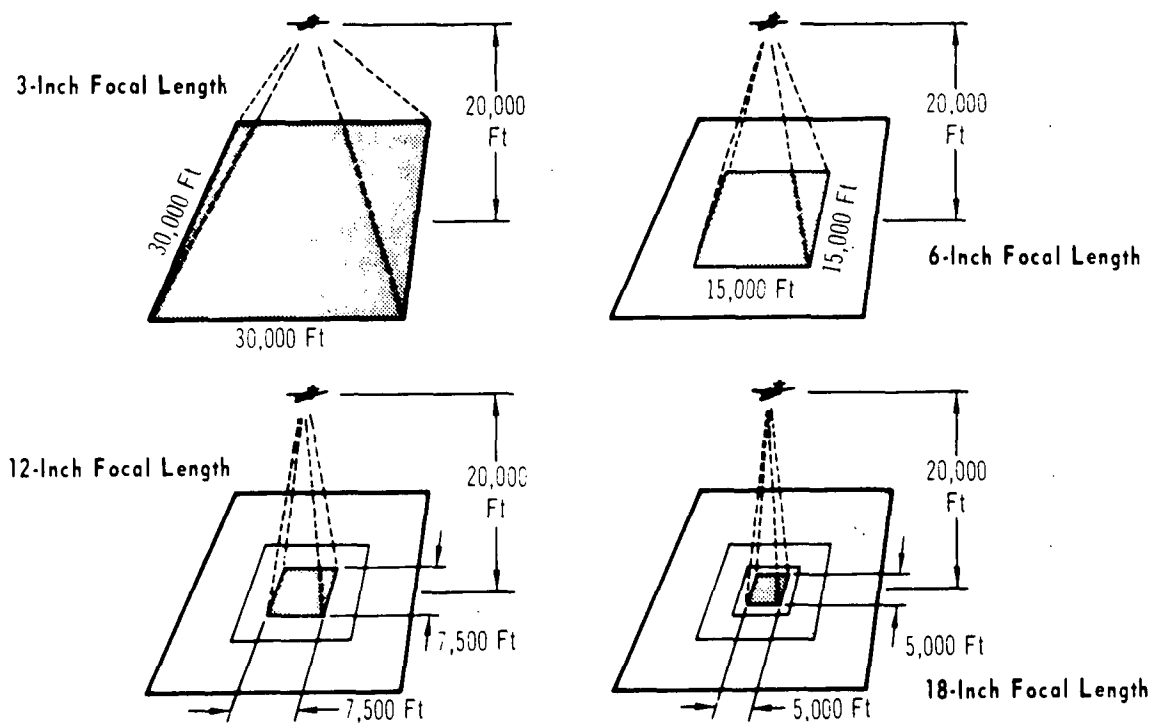


DIAGRAM B Effect of Focal Length on Scale and Ground Coverage

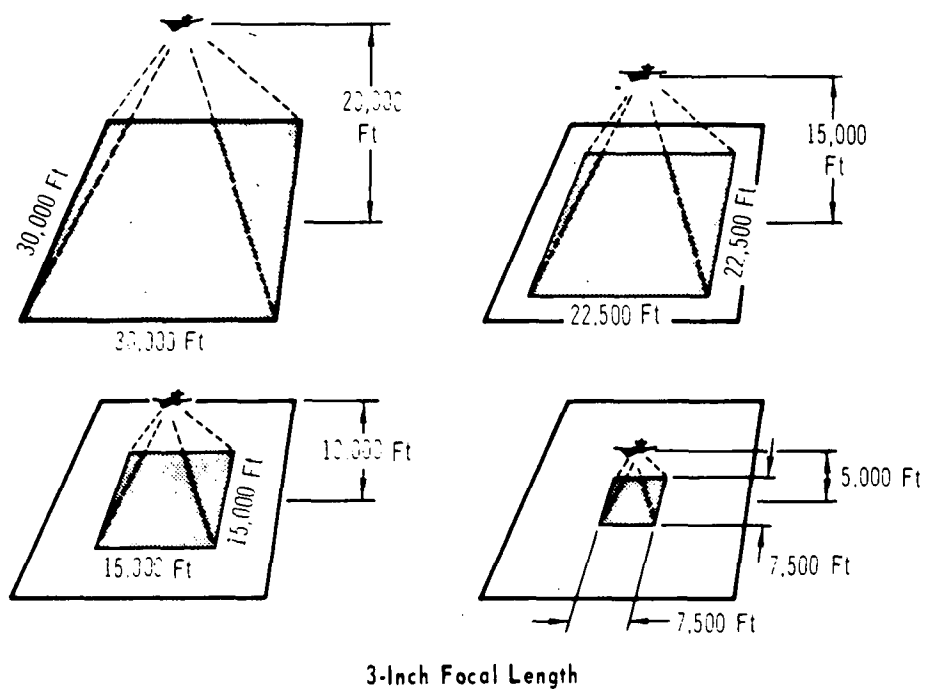


DIAGRAM C Effect of Altitude on Scale and Ground Coverage

APPENDIX B
TIME-DISTANCE DATA
24 APRIL 1973 FLIGHTS

Table B-1

Time-Distance Data for First Flight, 24 April 1973

Time	Δt (Min.)	Distance		Velocity		Heading	Distance		Velocity		Heading
		(m)	(ft)	(km/h)	(mph)		(m)	(ft)	(km/h)	(mph)	
11:37 11:44 11:51 12:01 12:13 12:22 12:29 12:36 12:43 12:50 <u>a/</u>	7 14 24 36 45 52 59 66 73 73	Surface					3 m (10 ft)				
		75	246	.64	.39	289°	94	310	.81	.50	285°
		75	246	.64	.39	272°	72	236	.62	.38	276°
		86	280	.51	.32	280°	90	295	.77	.48	282°
		96	315	.48	.29	276°	90	295	.77	.48	275°
		63	207	.42	.26	261°	70	231	.60	.37	264°
		59	192	.50	.31	298°	55	182	.48	.30	296°
		17	54	.14	.08	316°	28	93	.24	.15	298°
		105	345	.90	.55	296°	67	221	.58	.36	302°
		18	59	.15	.09	213°	19	64	.17	.11	198°
552	1811	.45	.28	280°	555	1820	.46	.28	280°		
11:37 11:44 11:51 12:01 12:13 12:22 12:29 12:36 12:43 12:50 <u>a/</u>	7 14 24 36 45 52 59 66 73 73	6 m (20 ft)					12 m (40 ft)				
		69	226	.59	.36	289°	36	118	.30	.19	296°
		57	187	.48	.29	259°	27	89	.23	.14	256°
		73	240	.62	.38	273°	30	98	.26	.16	250°
		72	236	.36	.22	259°	24	79	.20	.12	225°
		48	157	.32	.19	245°	16	52	.14	.09	180°
		28	92	.24	.14	285°	12	39	.10	.06	94°
		33	108	.28	.17	332°	16	52	.14	.09	157°
		50	164	.42	.26	241°	21	69	.18	.11	183°
		30	98	.13	.08	196°	28	92	.24	.15	155°
405	1329	.33	.20	265°	114	374	.09	.06	216°		

a/ Straight line between first and last position.

Table B-2

Time-Distance Data for Second Flight, 24 April 1973 (Night)

Time	Δt (Min.)	Distance		Velocity		Heading	Distance		Velocity		Heading
		(m)	(ft)	(km/h)	(mph)		(m)	(ft)	(km/h)	(mph)	
20:28 20:34 20:41 20:51 20:59 21:08 21:15 21:23 <u>a/</u>	6 13 23 31 40 47 55 55	Surface					3 m (10 ft)				
		34	110	.34	.21	203°	34	110	.34	.21	167°
		17	55	.14	.09	203°	47	154	.40	.24	210°
		82	268	.49	.30	222°	59	193	.35	.22	212°
		82	268	.61	.38	235°	98	323	.74	.46	219°
		144	472	.96	.60	115°	151	496	1.00	.63	220°
		48	157	.41	.26	250°	72	236	.62	.38	242°
		319	1047	2.39	1.49	215°	305	1000	2.28	1.42	209°
		706	2315	.77	.48	222°	742	2433	.81	.50	214°
		6 m (20 ft)					12 m (40 ft)				
20:28 20:34 20:41 20:51 20:59 21:08 21:15 21:23 <u>a/</u>	6 13 23 31 40 47 55 55	62	205	.62	.36	179°	42	138	.42	.26	170°
		56	185	.48	.30	208°	46	150	.39	.24	206°
		88	287	.58	.39	199°	48	157	.29	.18	223°
		77	252	.58	.38	226°	67	220	.50	.31	244°
		190	622	1.26	.78	224°	107	350	.71	.44	241°
		54	177	.46	.29	251°	119	390	1.01	.63	271°
		308	1011	2.31	1.43	213°	163	535	1.24	.76	213°
		801	2630	.87	.54	217°	521	1709	.57	.35	231°

a/ Straight line between first and last position.

Table B-3

Time-Distance Data for Third Flight, 24 April 1973 (Late Night)

Time	Δt (Min.)	Distance		Velocity		Heading	Distance		Velocity		Heading
		(m)	(ft)	(km/h)	(mph)		(m)	(ft)	(km/h)	(mph)	
23:37 23:44 23:53 24:03 24:13 24:22 24:32 24:41 24:51 <u>a/</u>	7 16 26 36 45 55 64 74 74	Surface					3 m (10 ft)				
		134	438	1.14	.71	273°	134	438	1.14	.71	271°
		168	552	1.11	.69	321°	170	558	1.12	.70	317°
		194	636	1.15	.72	325°	152	498	.90	.56	325°
		124	408	.74	.46	320°	137	450	.82	.51	317°
		102	336	.67	.42	14°	90	294	.59	.37	5°
		161	528	.96	.60	4°	126	413	.76	.47	12°
		135	444	.90	.56	0°	102	336	.67	.42	343°
		104	340	.62	.38	358°	126	413	.76	.47	17°
		972	3189	.79	.49	326°	876	2874	.71	.44	321°
23:37 23:44 23:53 24:03 24:13 24:22 24:32 24:41 24:51 <u>a/</u>	7 16 26 36 45 55 64 74 74	6 m (20 ft)					12 m (40 ft)				
		156	511	1.30	.82	275°	108	354	.92	.57	264°
		144	472	.94	.59	309°	132	433	.88	.54	308°
		151	494	.90	.56	331°	165	541	.99	.61	323°
		138	452	.82	.51	306°	111	364	.66	.41	308°
		126	413	.83	.52	335°	126	413	.84	.52	342°
		126	413	.74	.46	353°	120	393	.72	.44	343°
		145	474	.94	.60	334°	141	462	.94	.60	325°
		132	433	.79	.49	13°	141	462	.84	.52	344°
		978	3209	.79	.49	317°	948	3110	.77	.48	312°

a/ Straight line between first and last position.